# The distribution of p38(MAPK) in the sensorimotor cortex of a mouse model of Alzheimer's disease

A Thesis Submitted to the
College of Graduate Studies and Research
in Partial Fulfillment of the Requirements
for a Master's Degree
in Biological Psychiatry
Department of Psychiatry
University of Saskatchewan
Saskatoon

By
Tuo Zhao

# PERMISSION TO USE

In presenting this thesis in partial fulfillment of the requirements for a Master's degree from the University of Saskatchewan, I agree that the Libraries of this university make it freely available for inspection. I further agree that permission for copying of this thesis in any manner, in whole or in part, for scholarly purposes may be granted by Dr. Darrell D. Mousseau, who supervised my thesis work or, in his absence, by the head of the Department of Psychiatry at the University of Saskatchewan. It is understood that any copying, publication, or use of this thesis or parts thereof for financial gain shall not be allowed without my written permission. It is also understood that due recognition shall be given to me, to the Department of Psychiatry and to the University of Saskatchewan in any scholarly use which may be made of any material in my thesis.

Request for permission to copy or to make other use of material in this thesis in whole or in part should be addressed to:

Dr. Darrell D. Mousseau and/or
Head of the Department of Psychiatry
University of Saskatchewan
Saskatoon, Saskatchewan
Canada, S7N 5E5

# ABSTRACT

The p38 mitogen-activated protein kinase [p38(MAPK)] mediates responses to extracellular stressors. An increase in the phosphorylated form of p38(MAPK) [p-p38(MAPK)] has been associated with early events in Alzheimer disease (AD). Although most often associated with processes including apoptosis, inflammation and oxidative stress, p-p38(MAPK) also mediates beneficial physiological functions, such as cell growth, survival and phagocytosis of cellular pathogens. The presence of amyloid plaques [β-amyloid aggregates] is one of the hallmarks of AD-related pathology. As p38(MAPK) has been detected in the vicinity of amyloid plaques, we combined immunohistochemistry and stereological sampling to quantify the distribution of plaques and p-p38(MAPK)-immunoreactive (IR) cells in the sensorimotor cortex of 3-, 6- and 10-month-old TgCRND8 mice. This animal model expresses an AD-related variant of the human amyloid-β protein precursor (APP). The aggressive nature of this variant was confirmed by the appearance of both dense-core (thioflavin-S-positive) and diffuse plaques, even in the youngest mice. p-p38(MAPK)-IR cells were associated with both dense-core and diffuse plaques, but the age-dependent increase in the density of plaque-associated p-p38(MAPK)-IR cells was limited to dense-core plaques. Furthermore, the density of these dense-core plaque-associated cells was inversely correlated with the size of the core within the given plaque, which suggests a role for these microglia in restricting core growth. Parenchymal p-p38(MAPK)-IR cells were also observed in both wildtype and TgCRND8 mouse cortex. However, the density of these parenchymal cells remained constant, regardless of age or genotype. The majority of p-p38(MAPK)-IR cells were predominantly co-immunoreactive for the Macrophage-1 (CD11b) microglial marker, regardless of whether they were associated with plaques or localized to the parenchyma. This constitutive presence of p-p38(MAPK)-IR microglia in aging mouse brain is suggestive of a longitudinal role for this kinase in normal brain physiology. The plaque-associated pool of p-p38(MAPK)-IR microglia appears to restrict β-amyloid core development. This, as well as the non-pathological role of p-p38(MAPK) in parenchyma, needs to be considered when interpreting p38(MAPK)-dependent mechanisms in the context of both experimental and clinical AD.

# ACKNOWLEDGMENTS

First of all, I would like to express my sincere gratitude to my supervisor, Dr. Darrell Mousseau for his continuous professional support and supervision, throughout my Master's program. From the guidance of Dr. Mousseau, I not only developed the technical expertise associated with my project and knowledge of neuropsychiatry, but also learned the way to think independently. Dr. Mousseau is truly an excellent example of a great scientist. His patience and passion on science has always been inspiring and stimulating to me.

I also would like to thank the rest of my thesis committee for their support and guidance: Drs. Jennifer Chlan-Fourney, Xinmin-Li and Wolfgang Walz. I appreciate their insightful comments and encouragement. I am also thankful to my external examiner, Dr. William Roesler, for his insight and his feedback on this thesis.

Throughout my Master's training, I was most fortunate to work with my fellow graduate students: Ji Qi, Lewei Rui, Tamara Satram-Maharaj and my colleagues Paul Pennington Dr. Zhongjian Jiang and Dr. Zelan Wei. I thank them all for their kind help, stimulating discussions and all the fun we had. I would like express special thanks to Dr. Jennifer Chlan-Fourney for her patient teaching of the experimental techniques during the first year of my study.

Last but not least, I would like to thank my parents, the rest of my family and friends – they have always been supportive during every day of my 3-year study.

# TABLE OF CONTENTS

# LIST OF FIGURES

# LIST OF TABLES



# LIST OF ABBREVIATIONS

| | |
|---|---|
| AD: | Alzheimer's disease |
| APP: | Amyloid-β protein precursor |
| ATF: | Activating transcription factor |
| BrdU: | 5-bromo-2′-deoxyuridine |
| Cox: | Cyclooxygenase |
| CREB: | cAMP response element binding protein |
| DAB: | 3,3′-diaminobenzidine |
| ERK: | Extracellular signal-regulated kinase |
| GADD153: | Growth arrest and DNA damage inducible gene 153 |
| HSP27: | Heat shock protein 27 |
| IGF: | Insulin-like growth factor |
| IL-1: | Interleukin-1 |
| IR: | Immunoreactivity |
| JNK: | c-Jun $NH_2$-terminal kinases |
| MAK: | Mitogen-activated kinase |
| MAPKAPK: | MAPK-activated protein kinase |
| MAO-A: | Monoamine oxidase-A |
| MAPK: | Mitogen-activated protein kinase |
| MCC: | The mean number of cells per volume |
| MEF2A/2C: | Monocyte enhance factor 2A/2C |
| MKK: | MAPK kinase |
| MKKK: | MKK kinase |
| MNK: | MAPK-interacting kinase |
| NFT: | Neurofibrillary tangle |
| NGF: | Nerve growth factor |

| | |
|---|---|
| NHE-1: | $Na^+$-$H^+$ exchanger isoform-1 |
| PB: | Phosphate buffer |
| PBS: | Phosphate-buffered saline |
| PFA: | Paraformaldehyde |
| p-p38: | Phosphorylated form of p38 |
| Sap-1: | SRF accessory protein 1 |
| TAK: | TGF-β-activated kinase |
| TCR: | T cell receptor |
| TGF: | Transforming growth factor |
| TNF: | Tumor necrosis factor |
| TX: | Triton X-100 |

# 1. INTRODUCTION

## 1.1 Alzheimer's disease (AD)

### 1.1.1 Definition and classification of AD

Alzheimer's disease (AD) is the most common form of dementia [1]. This progressive, neurodegenerative and incurable disease was first described by the German psychiatrist Alois Alzheimer in 1906, and then was named after him [2]. Currently, AD is one of the most prevalent diseases related to aging [3]. In 2006, there were 26.6 million sufferers worldwide [4]. AD includes sporadic [late-onset] and early-onset forms of the disease. The sporadic form of AD is the most common and accounts for almost 90% of diagnosed cases [5]. The rate of incidence of AD is approximately 5% of people 65 years old and this rate doubles every 5 years thereafter [3, 5]. Almost 50% of people aged 85 years or older are affected by AD [5]. In contrast, cases of early-onset AD are usually those diagnosed before the age of 65 years. It is the less prevalent form of AD, accounting for only 5-10% of all cases [4]. Furthermore, approximately half of the cases of early-onset AD are familial AD (FAD), which implicates a genetic predisposition [6]. Three predisposition genes include those coding for the proteins presenilin-1 (*PS1*), presenilin-2 (*PS2*), and amyloid-β protein precursor (*APP*) [7].

### 1.1.2 Characteristics of AD

Although the course of AD is unique for every individual, there are still many common symptoms. Generally, based on the extent of progressive cognitive and functional impairment, the disease can be divided into four stages, with an increasing degree of dementia: (a) pre-dementia, (b) early, (c) moderate, and (d) advanced [8, 9]. The cognitive and behavioral changes associated with the first stage are most often mistaken as changes relating to aging or stress [10]. The most complex of daily living activities can be affected in this very early stage and memory loss can be determined using the appropriate neuropsychological testing [9, 11]. Further impairment of thinking and memory shows up during the second stage of AD**.** In a small portion of the patients, difficulties with language, perception and execution of movements are more prominent than memory problems [8]. At the third (or moderate) stage, a person with AD is unable to perform the most common activities of daily living. Speaking and writing skills are

progressively lost. At the same time, memory problems further worsen and long-term memory becomes impaired [8, 12]. During the fourth (or advanced) stage, patients are completely dependent on caregivers. The ability to speak is completely lost and muscle mass and mobility deteriorate; at this stage, patients are bedridden and lose the ability to feed themselves. Although AD cannot itself directly cause the death of people, it is considered a terminal illness as it predisposes to external factors that facilitate infections such as pneumonia and pressure ulcers, which ultimately precipitate death [8, 13].

### 1.1.3 Pathology of AD

The neuropathological changes of AD include neuronal degeneration, the presence of intracellular neurofibrillary tangles (NFT) and formation of extracellular amyloid (senile) plaques (Figure 1) [1].

Currently, the '*tau*' and the 'beta-amyloid' hypotheses are the most popular theories used to explain AD [14]. The '*tau*' hypothesis proposes that hyperphosphorylation of the microtubule-associated protein *tau* causes it to dissociate from the cytoskeleton and aggregate with other threads of *tau* to form paired helical filaments (PHFs), which eventually form the intracellular NFTs [15].When this occurs, intracellular transport is compromised, resulting in the malfunction of biochemical communication between neurons. The death of the cell is then imminent [16].

The 'beta-amyloid' hypothesis proposes that the amyloid plaques are the fundamental cause of the disease [17]. The beta-amyloid (Aβ) toxic peptide is the major constituent of the amyloid plaque and these plaques/aggregates are often most evident in limbic and association cortices of the AD brains [1, 14]. Elevated levels of Aβ then induce microglial activation and proliferation, and promote the release of proinflammatory cytokines, such as interleukins (IL) and tumor necrosis factors (TNF) [14].

### 1.1.4 The Amyloid Protein Precursor

The Aβ peptide contains 39 to 43 amino acids and is generated following the cleavage of the amyloid precursor protein (APP) molecule [18]. The *APP* gene is located on chromosome 21 and the APP protein is an integral transmembrane protein expressed

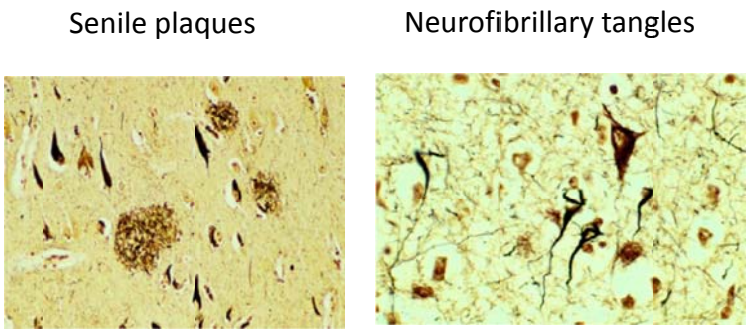


**Figure 1. Examples of amyloid (senile) plaques and neurofibrillary tangles in AD brain.** *(left)* The senile plaque is the hallmark of AD-related pathology. It is formed by a concentration-dependent aggregation of the highly hydrophobic (fibrillogenic) amyloid peptide. *(right)* Neurofibrillary tangles result from the disruption of the cytoarchitecture as a consequence of the hyperphosphorylation of the microtubule-associated *tau* protein.

in many tissues and concentrated in the synapses of neurons [19, 20]. APP can be processed by three enzymes, e.g. α-, β- and γ-secretases [21]. Under normal conditions, APP is cleaved by α-secretase between residues 16 and 17 within the Aβ peptide region to release sAPPα [22] (Figure 2). Under certain conditions, successive action of the β- and γ-secretases generates the Aβ peptide (note that cleavage by α-secretase, given that it cleaves the APP protein within the Aβ sequence, precludes generation of the intact Aβ peptide). The AD-related mutations in APP, which are often near the β-secretase site, promote cleavage by β-secretase and thus alter the availability of Aβ. β-secretase cleaves APP between residues 596 and 597, thus shedding the N-terminus of APP and leaving the C-terminus of APP (C99; because of the number of residues it contains) [23]. The membrane-bound C99 can then be cleaved by γ-secretase to generate Aβ peptides of varying length (e.g. 39-43 amino acids) [24] (Figure 2). The most common forms of Aβ are $A\beta_{40}$ and $A\beta_{42}$. The $A\beta_{42}$ peptide is more fibrillogenic and because of its tendency to aggregate into plaques, it has been historically associated with AD. In transgenic animals, the APP mutations associated with AD decrease the production of $A\beta_{40}$ or increase the production of $A\beta_{42}$ [25], both of which leads to peptide aggregation and plaque formation.

### 1.1.5 Classification of amyloid plaques

The accumulation of the toxic Aβ peptide plays a central role in AD-related pathology and amyloid plaque formation [26]. Amyloid plaques are variable in both shape and size in the AD brains and individual tissue sections, but the average size is around 50 μm [27]. Two types of plaques, designated as (a) 'dense-core' or (b) 'diffuse', are detected during amyloid deposition [14]. 'Dense-core' plaques are formed by the fibrillar/β-sheet conformation of Aβ and usually contain a central amyloid core. Much of the fibrillar Aβ found in the 'dense-core' plaques is $A\beta_{42}$, since this longer and more hydrophobic form is prone to aggregation. However, the other species, $A\beta_{40}$, can be also co-detected with $A\beta_{42}$ in this kind of plaque [28]. The diameter of 'dense-core' plaque in brain sections varies widely from 10 to >120 μm and the density of Aβ fibrils within the core (i.e. how compact they are) also shows great variability between plaques [14].

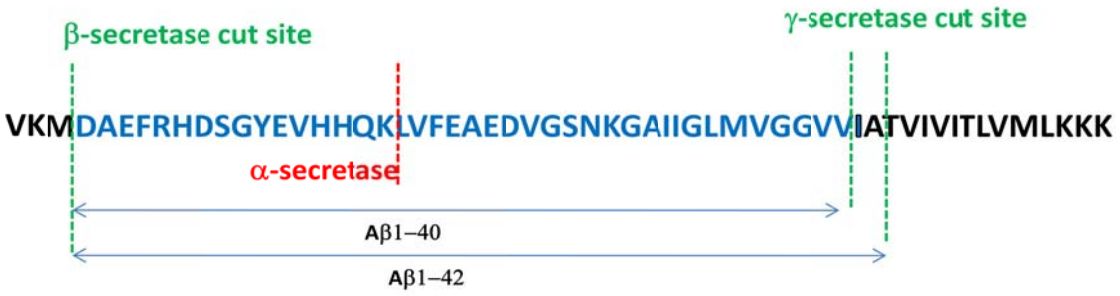


**Figure 2. The amyloid-β protein precursor (APP) is cleaved by multiple proteolytic events.** The portion of the APP amino acid sequence spanning V669 to K726 [the numbering of residues is based on APP770] is shown here. APP can be cleaved by α-, β- and/or γ-secretase between different residues to give release fragments. The sequential cleavage by β- and γ-secretases releases the $A\beta_{40}$ and $A\beta_{42}$ fragments (highlighted in blue) (image adapted from Li [29]).

Currently, the time required to develop 'dense-core' plaques in humans is unknown, although it is assumed that months or years are needed for the gradual development of these lesions [28]. Moreover, the 'dense-core' plaques are associated with degenerative neural structures and an abundance of microglia and astrocytes. These microglia usually surround the outside of the plaque and their processes sometimes extend into the amyloid core [26]. The other kind of plaque is defined as 'diffuse' [30]. 'Diffuse' plaques are predominantly comprised of the $A\beta_{42}$ peptide, with no or little $A\beta_{40}$ immunoreactivity, and differ from 'dense-core' plaques that are formed by a mixture of $A\beta_{42}$ and $A\beta_{40}$ [31]. Furthermore, Aβ deposits in the 'diffuse' plaques lack the fibrillar and compressed conformation that is characteristic of the Aβ deposits in the 'dense-core' plaques; it is the absence of a clearly defined fibrillar and compacted center core that led to the 'diffuse' label for this category of plaques. In addition, there is very little or no detectable neural degeneration in or around most of these 'diffuse' plaques [32, 33]. These observations suggest that the 'diffuse' plaque is quite distinct from the 'dense-core' plaque in the AD brain [34]. However, another competing hypothesis proposes that 'diffuse' plaques represent immature lesions, which are the precursors to the 'dense-core' plaques. This hypothesis is supported by the evidence that in the same regions of AD patients, there is a mixture of 'diffuse' and 'dense-core' plaques, and 'diffuse' plaques develop before the fibrillar 'dense-core' plaques in transgenic mice expressing mutated human APP [14, 34].

### 1.1.6 AD-related animal models

The use of animal models of AD is essential to the research of pathology and to the validation of preclinical and therapeutic approaches [35]. The following is a brief description of certain of these models. The Aβ peptide and tau protein are the major constituent of amyloid plaques and NFTs, respectively [1] and have been used to generate mouse models of AD. The Tg2576 mouse was the first APP transgenic model and it expressed APP containing the Swedish mutation (K670N/M671L) [the KM residues are immediately upstream of the Aβ peptide fragment in APP; see Figure 2]. In the brains of this mouse model, transgenic APP was 5.6 times more than endogenous APP, and compared to wildtype littermates, a 5-fold increase in Aβ40 and 14-fold increase in Aβ42 were observed [36]. TgCRND8 is another commonly used APP transgenic mouse model

that overexpresses both the Swedish (as above) and the Indiana (V717F) mutations. This dual substitution is very aggressive and results in elevated amounts of Aβ and the aggregation of Aβ into plaques at a very early age [37, 38]. Another useful model is the PS-1(M146V) mouse which overexpresses an AD-related PS-1 variant [39]. PS-1 is known as the central catalytic component of the γ-secretase complex and mutations in PS-1 not only cause the increased amount of Aβ42, but are also linked to early-onset familial AD [40, 41]. Recently, mice carrying mutated form of APP as well as PS-1, in addition to mutated tau-related genes, have been made available, e.g. the $APP_{SW}/TAU_{P301L}/PS\text{-}1_{M146V}$ mouse model. In this 'triple transgene' mouse model, Aβ and tau expression are doubled, and both amyloid plaques and NFTs are developed at an early age [42].

## 1.2 Mitogen-activated Protein Kinases (MAPKs)

### 1.2.1 Brief overview of MAPKs

Protein kinases transfer phosphate groups to the specific proteins as a means of regulating the function of these proteins [43]. Among the large group of protein kinases, the family of MAPK is well characterized. In specific substrates, it is serines and threonines that are the preferred amino acids targeted for phosphorylation by MAPKs [44]. Activation of MAPKs occurs via a series of 'upstream' events that is termed the 'MAPK cascade'. Each cascade consists of three levels of activation, with each level being represented by a specific kinase; MAPK, MAPK kinase (MKK, MEK) and MKK kinase (MKKK). A MKKK that is activated by extracellular stimuli phosphorylates a MKK on its serine and threonine residues; in turn this MKK activates a MAPK by phosphorylating specific threonine and tyrosine residues [45]. The specificity of the phosphorylation of MAPKs is based on the 'T*X*Y' (T=threonine; *X*=any amino acid; Y=tyrosine) motifs found in the different MAPKs (Figure 3). The phosphorylation of both threonine and tyrosine residues in a given MAPK is required for full activation of MAPKs and [partial/full] inactivation will occur if either residue is dephosphorylated by a phosphatase [46]. The MAPK cascade is a highly conserved signal transduction pathway from yeast to mammalian cells [47]. It responds to many different external stimuli, which induce specific MAPK cascades to phosphorylate particular downstream

kinases from MKKK, MKK to MAPK and its substrates [48]. The various biological functions are determined by the diverse and specific cells, and as such MAPK cascades are involved in a wide range of cellular activities, including cell growth, differentiation, migration, survival, inflammation and apoptosis [45].

### 1.2.2 MAPKs subfamilies

Three main subgroups of the MAPK family are well characterized: extracellular signal-regulated kinases (ERKs), c-Jun $NH_2$-terminal kinases (JNK) and p38(MAPK) [49]. Sequence comparison reveals all the members in MAPK subfamilies share 40-45% amino acid identity, and the 'TXY' motifs targeted for phosphorylation by specific upstream MKKs in the three subfamilies are 'TEY' (single-letter code for threonine, glutamic acid, tyrosine) in ERKs, 'TPY' (threonine, proline, tyrosine) in JNKs, and 'TGY' (threonine, glycine, tyrosine) in p38(MAPK). These motifs are located in a loop structure of the respective MAPKs close to the active site [50, 51].

ERK1 and ERK2 were the first cloned MAPKs [52]. Many different stimuli (e.g. growth factors, cytokines, ligands for heterotrimeric G protein-coupled receptors and viral infection) can activate the ERK pathway. In the typical ERK/MAPK cascade, MKKK is phosphorylated by small G protein Ras, and the MKK1/2 and ERK1/2 are then activated subsequently [51, 52]. Classically, the ERK pathway is involved in the control of cell proliferation, differentiation and mitosis [53]. In addition to ERK1/2, ERK3/4/5/7 and 8 have been cloned recently and are associated with diverse biological functions [54].

Both JNK and p38(MAPK) cascade are activated by environmental stressors, such as UV radiation, X-rays, heat shock, osmotic shock as well as inflammation induced by cytokines, including interleukin-1 (IL-1) and tumor necrosis factor (TNF). Three members, JNK1, JNK2 and JNK3, are included in the JNKs subfamily [55]. In the JNK signaling pathway, although the activation of MKKKs is too complicated to be properly characterized (because of a diversity of various upstream stimuli), the activation of JNKs by MKK4 and MKK7 is well understood [55, 56]. Because this thesis is focused on p38(MAPK), this signaling pathway will now be examined in more detail.

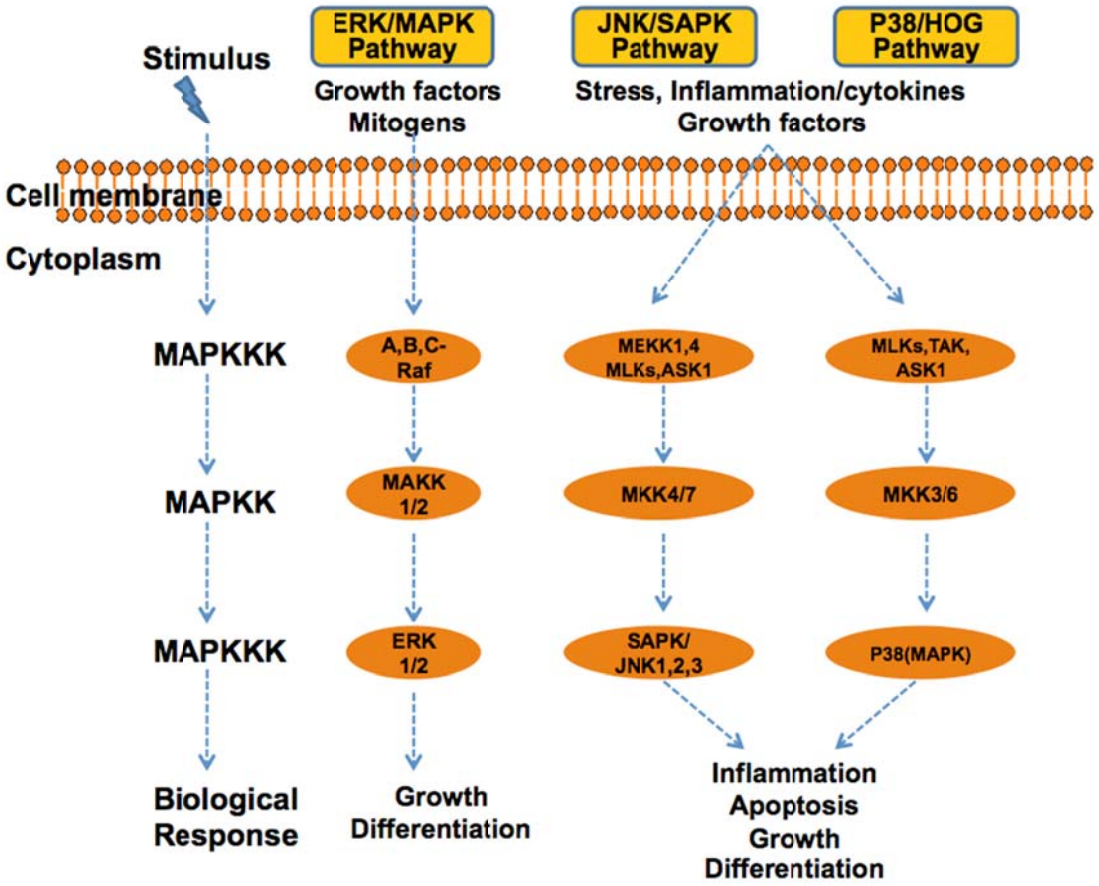


**Figure 3. Schematic of MAPK cascades.** The generic 'MAPK cascade' is shown on the left and examples of the signaling molecules involved in the three MAPK subfamilies are also listed. Focusing on the p38(MAPK) pathway (**right**), a possible sequence might include: TGF-β-activated kinase (TAK) is activated by the growth factor TGF-β binding to its receptor. This kinase would phosphorylate serine/threonine residues in MKK3 or MKK6. Once activated, MKK3/MKK6 would phosphorylate the dual phosphorylation motif, e.g. pTGpY (phospho-threonine, glycine, phospho-tyrosine), in p38(MAPK). The activated p38(MAPK) would then target one of many substrates to induce a specific cellular response such as inflammation, apoptosis, growth or differentiation. The specific cellular response might depend on the different external stimuli, various activated upstream kinases and the 'cross-talk' between pathways. (image adapted from Bijl-Westra [57]).

### 1.2.3 Brief overview of p38(MAPK) signaling

p38(MAPK) is the most recently identified, but also the most studied, MAPK of the three main MAPK subfamilies [58]. It was originally identified as a 38-kDa kinase rapidly phosphorylated in response to endotoxic lipopolysaccharide [59]. Four isoforms of p38(MAPK) have been reported and labeled as α, β, γ and δ. All four p38(MAPK) homologues share approximately 60-75% identity in their amino acid sequence, yet each isoform has its unique distribution, expression, activation and substrate affinity, all of which results in their varied functions [60-62].

### 1.2.4 Localization of p38(MAPK)

Among the four isoforms of p38(MAPK), *p38(MAPK)-α* and *β* genes are broadly expressed. p38(MAPK)-α was the first identified and it is expressed ubiquitously. A high level of expression of p38(MAPK)-β has been observed in the brain and heart [60, 63]. p38(MAPK)-γ and -δ are expressed in different tissues: p38(MAPK)-γ is mainly expressed in skeletal muscle, while p38(MAPK)-δ is more in peripheral organs, such as lung, kidney, testis, pancreas, ovary, adrenal and pituitary gland [64, 65]. All of the p38(MAPK) isoforms can be detected in both nucleus and cytoplasm as studies have demonstrated that when cells respond to external stimuli, p38(MAPK) can translocate from cytoplasm to the nucleus. However, some p38(MAPK) are able to activate specific cytoplasmic substrates and do not require a nuclear translocation event [66, 67].

### 1.2.5 The p38(MAPK) pathway

The extracellular stimulation of the p38(MAPK) pathway is similar to that described above for JNKs [55]. Studies have demonstrated that inflammatory cytokines, such as IL-1, TNF, and G-protein-coupled receptor agonists are all able to trigger p38(MAPK)-mediated phosphorylation events [48]. In addition, many growth factors, including nerve growth factor (NGFs), insulin-like growth factor (IGFs) and transforming growth factor (TGFs) can activate p38(MAPK) [68] and environmental stressors, such as UV radiation, X-rays, heat shock and osmotic shock have also been implicated in its activation [55]. However, the various stimuli induce different upstream kinases to be

phosphorylated in diverse cell types, and the different isoforms of p38(MAPK) can then be activated by the various phosphorylated upstream kinases [48]. After the extracellular stimulation, low molecular weight GTP-binding protein, such as Rho family, Rac and Cdc42 as well as G-protein-coupled receptors all contribute to the upstream activation of MKKKs. The activated MKKKs then trigger the phosphorylation of the downstream MKK and the specific MAPK [69].

The high-affinity MKK3/6 and low-affinity MKK4 are involved in p38(MAPK) activation [70]. MKK6 has been found to activate all four p38(MAPK) isoforms, whereas MKK3, which is 80% homologous to MKK6, cannot effectively phosphorylate p38(MAPK)-β, but can phosphorylate p38(MAPK)-α, -γ and -δ [71]. MKK4 has been implicated in the activation of p38(MAPK)-α [70]. Thus, diverse stimulation and different upstream kinases lead to isoform-specific p38(MAPK) phosphorylation, and this will further cause several distinct p38(MAPK) substrates to be activated (Figure 3) [48].

### 1.2.6 Substrates of p38(MAPK)

Inhibition of p38(MAPK) using pharmacological approaches or conditional knock-out animals allows for the identification of the physiological substrates for p38(MAPK). There are many substrates in both the nucleus and cytoplasm, suggesting multiple physiological effects can be induced based on subtle actions and interactions centered on the molecules involved in p38(MAPK) pathways [48]. The first kind of substrates are the protein kinases phosphorylated by activated p38(MAPK), termed MAPK-activated protein kinases (MAPKAPKs). The mitogen-activated kinases (MAKs) and stress-activated kinases (MSKs), MAPK-interacting kinases (MNKs) and MAPKAPK2, 3 and 5 all belong to the MAPKAPKs family, and depending on the signal from the upstream cascade, these MAPKAPKs can phosphorylate many other molecules to trigger diverse cellular responses [72]. The second category of p38(MAPK) substrates includes a number of important transcription factors, such as activating transcription factor (ATF)1, 2 and 6, SRF accessory protein 1 (Sap1), growth arrest and DNA damage inducible gene 153 (GADD153), p53, C/EBP-β, monocyte enhance factor 2A/2C (MEF2A/2C), MITF1, DDIT3, ELK1, NFAT, E1K-1, NFκB, Ets-1 and high mobility group-box protein 1 [50, 72, 73]. In addition, other types of substrates, such as Cpla2,

$Na^+$-$H^+$ exchanger isoforms-1 (NHE-1), *tau*, kertin 8, stathmin and the hyperpolarization-activated cyclic nucleotide-gated channel have also been identified [74]. Moreover, proteins such as tyrosine hydroxylase, cAMP response element-binding protein (CREB), heat shock protein 27 (HSP27) and tritetraproline can also be activated indirectly by p38(MAPK) (Figure 4) [50, 74, 75]. Based on the great number of substrates, the p38(MAPK) cascade may be associated with multiple biological functions as diverse as inflammation, oxidative stress, apoptosis, cytokine production, cell growth, proliferation, differentiation, survival, regulation of gene expression at transcriptional level and cytoskeletal reorganization [48].

### 1.2.7 The physiological and pathological role of p38(MAPK)

#### 1.2.7.1 p38(MAPK) and inflammation

The p38(MAPK)-α isoform is expressed in many cell lines involved in inflammation and is primarily responsible for regulating proinflammatory responses [76]. Once p38(MAPK) is phosphorylated [p-p38(MAPK)], its downstream substrates can induce inflammatory cytokines, such as IL, TNF and cyclooxygenase (COX) [69]. For example, the capacity of IL-1-induced IL-6 production and activation of MAPKAP-K2 are reduced in embryonic stem cells taken from the p38(MAPK)-α null mice when exposed to chemical stress [77]. More importantly, levels of IL-6 and TNF are also decreased in MAPKAP-K2-deficient mice [78]. Therefore, the p38(MAPK)/MAPKAP-K2 pathway is crucial for inflammatory cytokine signaling and production [69]. The loss of expression of the inflammatory cytokines is thought to be mediated via mechanisms involving transcription and translation that are regulated by the p38(MAPK) pathway [69]. The transcription and translation of IL-1 and TNF mRNA are controlled by proteins called AU-binding proteins. These proteins always occupy the AU-rich regions in the 3′-untranslated region, which can be found in IL-1 and TNF mRNA [79]. Normally, translation and transcription are blocked by the AU-binding protein and subsequently suppress the synthesis of IL-1 and TNF [80, 81]. However, when AU- binding proteins are phosphorylated by the p38(MAPK)/MAPKAP-K2, they can be released from the binding site of AU-rich regions in the RNAs. Therefore, once the AU-binding proteins are phosphorylated either directly by p38(MAPK) or indirectly by MAPKAP-K2, the

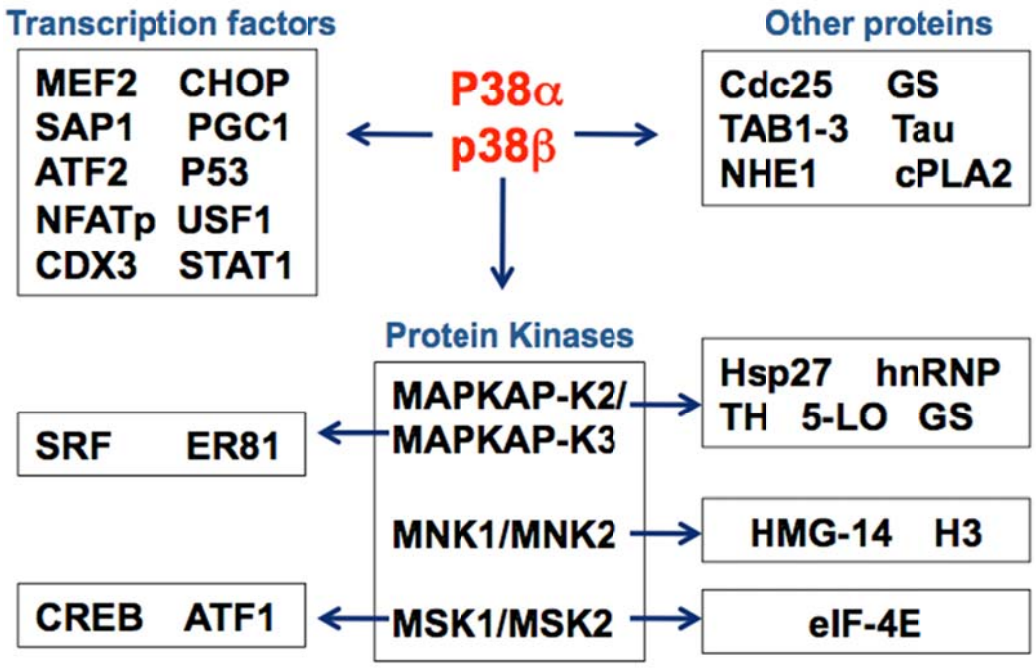


**Figure 4. Direct and indirect substrates of p38(MAPK).** p38(MAPK) is able to activate its target protein directly and also activates downstream proteins via the phosphorylation of protein kinases such as MAPKAP-K2/3, MNK and MSK. Activation of these substrates in both the cytoplasm and nucleus plays an important role in mediating cellular functions and maintaining normal physiological status. For example, the factors on the left side influence transcriptional regulation, whereas the proteins on the right side participate in specific cellular functions, such as cell cycle progression, chromatin remodeling, mRNA translation and stability and cytoskeleton reorganization metabolism. (image adapted from Cuenda and Rousseau [82]).

inflammatory cytokines, IL-1 and TNF, are induced and secreted [80, 81, 83].

#### 1.2.7.2 p38(MAPK) and cellular differentiation

p38(MAPK) plays a critical role in cellular differentiation, with myogenic differentiation being the best characterized. An increasing number of muscle-specific genes are expressed during the process of myoblast conversions to differentiated myotubes *in vivo*, and this process can be observed in cell culture. In these cell lines, the persistent activation of p38(MAPK) results in the enhanced expression of related genes, which accelerates the formation of myotubes [84, 85]. However, if the cells are treated with p38(MAPK) inhibitors, both myogenic progression and the expression of muscle-specific genes are blocked [86]**.** In another context, p38(MAPK) has been associated with enhancing neuronal differentiation via 'crosstalk' with other factors and kinases. The rat preneuronal pheochromocytoma PC12 cell line is well-characterized for the study of differentiation [87]. Using Nerve Growth Factor (NGF) to stimulate the cells and activate the MAPK pathways, both p38(MAPK) and ERK are activated, and cells stop multiplying and start to extend branching processes [88]. This effect can be explained as the 'crosstalk' (*def.*: in cell signaling, the term 'crosstalk' refers to the mechanism by which a condition can activate multiple responses and/or a 'signal' can be shared between different signalling pathways); crosstalk causes ERK and p38(MAPK) pathways to be activated by the same upstream kinase MKK following NGF stimulation [89]. Later on both the ERK and p38(MAPK) phosphorylate the transcription factor CREB, which can determine NGF-induced cell fate. Under the regulation of CREB, PC12 cells cease proliferation and begin differentiation [90].

#### 1.2.7.3 p38 and cell migration

By using a pharmacological p38(MAPK) inhibitor, another physiological role of p38(MAPK) in cell migration has been revealed. In a corneal wound healing model, two paracrine growth factors, e.g. hepatocyte growth factor and keratinocyte growth factor, induced the activation of p38(MAPK) pathway and a concurrent nuclear accumulation of phosphorylated p38(MAPK) in corneal epithelial cells. Treatment with the p38(MAPK) inhibitor SB203580 eliminates the activation and nuclear accumulation of p38(MAPK),

and the migration of epithelial cells is also blocked [91, 92]. The mechanism is thought to rely on the activation of the p38(MAPK) pathway associated with the expression of integrin, which leads to the epithelial-mesenchymal transition. In this case, p38(MAPK) may also regulate cell adhesion via the expression of paxillin, which is essential for cell migration [93-95]. In addition to numerous growth factors, cell migration also depends on cytoskeleton reorganization by the p38(MAPK) pathway. Indeed, inhibition of the p38(MAPK)/MAPKAPK2 pathway prevents cell migration by interrupting cytoskeleton polymerization [96].

#### 1.2.7.4 p38(MAPK) in apoptosis and cell survival

The cellular responses to p38(MAPK) signalling are diverse and complicated. The activation of p38(MAPK) cascades has been shown to promote cell death, whereas, under different condition, this cascade is also known to paradoxically enhance cell survival [97, 98]. In $CD4^{+}$T cells, the p38(MAPK) pathway is initiated by T cell receptor (TCR) ligation [99] and activation of the upstream kinases MKK3/6. MKK3 and MKK6 mediate T cell apoptosis, presumably through the phosphorylation of p38(MAPK) [100]. This hypothesis has been supported by the anti-CD3 mouse antibody-induced T cell apoptosis. The apoptosis can be blocked by treatment with the p38(MAPK) inhibitor SB203508 [101]. However, p38(MAPK) signalling may also help to prevent apoptosis. Studies reported that the apoptosis of activated macrophages is induced, while the amino-terminal extension of MKK3 and MKK6 are cleaved by the bacterium *bacillus anthracis* generated lethal factor. However, once the cells persistently express the cleavage form of MKK3 and MKK6, they are no longer vulnerable to the bacterium *bacillus anthracis*-induced apoptosis [99, 102]. Studies even revealed the duration of p38(MAPK) activation can determine whether induction or prevention of apoptosis occurs. In TNF-induced apoptosis, the activation of p38(MAPK) and JNK activation are divided into two phases. In the first phase, early activation of p38(MAPK) and JNK support the cell survival, whereas the activation of p38(MAPK) and JNK in the later phase is related to caspase-dependent apoptosis [103, 104]. Thus, p38(MAPK) signalling can determine both cell apoptosis and survival, but the ultimate outcome depends on the context as well as on the

combination of the specific extracellular stimuli, the upstream kinases involved and the duration of activation.

Three pathologies in which p38(MAPK) has been implicated, namely cancer, cardiovascular dysfunction and Alzheimer/s disease (AD), will now be examined.

### 1.2.7.5 p38(MAPK) in cancer and cardiovascular dysfunction

One new role of p38(MAPK) that has been observed in recent years is its participation in cancer and tumor development. Inhibition of the p38(MAPK) cascade induces tumour development and metastasis. In contrast, overexpression of p38(MAPK) prevents tumourigenesis [82, 105], potentially through its role in cell proliferation and in regulating cell cycle at G0, G1/S and G2/M transitions [106]. Meanwhile, p38(MAPK) pathway also mediates DNA damage checkpoints function, which is a mechanism to monitor the cell division. In addition, the p38(MAPK) cascade can also promote or inhibit, in a context-dependent manner, the activation of several oncogenes [107, 108]. p38(MAPK) is being considered as a potential target in cancer and tumour therapies [109].

Two causes of cardiovascular dysfunction are (a) hypertension-induced pressure overload cardiac hypertrophy and (b) ischemic injury induced cardiomyocyte apoptosis and necrosis [82, 110]. The p38(MAPK) upstream kinases MKK3 and MKK6 were overexpressed in cardiomyocytes, which caused significant increase of hypertrophy responses. This result suggests that p38(MAPK) mediates to the cardiac hypertrophy [110, 111]. During ischemia in perfused heart, the p38(MAPK) cascade can be activated by the reactive oxygen species generated from the mitochondria. Inhibition of p38(MAPK) activity protects apoptosis and necrosis induced by hypoxia and can prevent cell death during ischemia reperfusion [112, 113].

### 1.2.7.6 The role of p38(MAPK) in AD

p38(MAPK), particularly the phosphorylated form of p38(MAPK), is often expressed in vulnerable regions of AD brain, such as cortex and hippocampus [114, 115]. Moreover, p38(MAPK) has been suggested to contribute to the formation of the hyperphosphorylated *tau* (neurofibrillary tangles; NFTs) and amyloid plaques, as well as

other AD-related proteins [116-118]. In AD, more than thirty serine-threonine residues are phosphorylated and almost a half of the phosphorylated sites in *tau* are serine-threonine residues [82]. Therefore, it is reasonable to suppose that the kinases of the MAPK family play a crucial role in *tau* phosphorylation [117, 119]. In recent years, through the use of [$^{32}$P]-labeled ATP and phospho-specific antibodies, a number of p38(MAPK) phosphorylated residues in *tau* have been identified. Moreover, it has been demonstrated that *tau* is a stable substrate for p38(MAPK), especially for its p38(MAPK)-δ and -γ isoforms [120]. The phosphorylation of *tau* by p38(MAPK) results in the inability of *tau* to properly control microtubule assembly. Additionally, overexpression of p38(MAPK) in neuronal cells promotes *tau* phosphorylation and dissociation of *tau* from the cytoskeleton to ultimately promote NFT formation. Thus, p38(MAPK) regulates the hyperphosphorylation of *tau* in response to cellular stress [120, 121].

p38(MAPK) may influence AD progression by regulating other AD candidate protein activities, such as monoamine oxidase A (MAO-A) [116]. MAO-A is an important enzyme involved in the degradation of neurotransmitters, such as serotonin, dopamine and norepinephrine, and generates $H_2O_2$ as a reaction by-product [122]. Its role in modulating neurotransmitter availability makes MAO-A a major player in the neurobiology of depression. In addition to depression, MAO-A also plays a significant role in aging and age-related cognitive and mood disorders, such as learning, memory, cognition and sleep regulation. Interestingly, a link between a lifetime history of major depression and AD has been observed [123, 124]. Depressed patients have more amyloid plaques and NFTs in hippocampus and also people with major depression tend to be more likely to have a rapid decline into AD [125]. If MAO-A is contributing to depression in these patients, then this suggests that MAO-A might play a key role in the early neurochemical changes occurring in AD. Recently, an association between p38(MAPK) and MAO-A was proposed. Indeed, the inhibition of p38(MAPK) promotes MAO-A activity and MAO-A-sensitive toxicity in neuronal cell lines, which causes cell death. This may be induced by MAO-A-dependent oxidative stress and inflammation. However, overexpression of phosphorylated p38(MAPK) results in a decrease in MAO-A activity. As such, the regulation of MAO-A activity by p38(MAPK) could reduce MAO-A-

induced oxidative stress and inflammation in the early stages of AD [116].

A role for p38(MAPK) in AD has also been associated with amyloid plaque formation and development [118]. As mentioned before, the major amyloid plaque component Aβ induces microglial activation and causes the elevation in levels of pro-inflammatory cytokines [14]. Meanwhile, one of the biological functions of p38(MAPK) is regulating the biosynthesis and expression of the pro-inflammatory cytokines [69, 76]. Therefore, both Aβ and p38(MAPK) are believed to contribute to the amyloid plaque formation and development [126]. In the cortex and hippocampus of AD-related amyloidosis animal models, phosphorylated p38(MAPK)-immunoreactive microglia and astrocytes can be observed in the vicinity of amyloid plaques [127, 128]. This phenomenon is thought to result from the presence of Aβ within the plaques and its ability to stimulate the nearby microglia and astrocytes, or even neurons; these cells then induce an elevated level of inflammatory cytokines in a p38(MAPK)-dependent manner. Ultimately, the inflammation may play a role in exacerbating the pathology of AD [114].

### 1.3 Project hypothesis

The enzyme p38(MAPK) is a critical candidate protein in the cellular responses observed during AD; these involve inflammation and oxidative stress. It is because of its association with such responses that p38(MAPK) is most often thought of as being harmful. However, although p38(MAPK) has always been associated with apoptosis *in vitro*, its role in neuronal apoptosis in *vivo* remains ambiguous. Indeed, p38(MAPK) is constitutively activated in the cortex, hippocampus and cerebellum in normal conditions, and p38(MAPK) signaling has been shown to enhance cell growth, differentiation, survival [99, 129-132]. Moreover, p38(MAPK) activation has been observed in early stages of AD, when markers of apoptosis are uncharacteristically absent [133]. In the TgCRND8 mouse model of AD-related amyloidosis, amyloid plaque-associated cells that are immunoreactive for activated stress-associated protein kinases, e.g. JNK and the phosphorylated form of p38(MAPK) [p-p38(MAPK)], have been observed in the neocortex and hippocampus [114, 115, 133].

Given these various observations, **the hypothesis of this thesis is that p38(MAPK) exerts beneficial effects in [a model of] AD-related pathology, specifically by regulating amyloid plaque formation and development.**

### 1.4 Aim of the thesis project

What the exact role of p-p38(MAPK) plays in the AD brains, and whether p-p38(MAPK) is harmful or beneficial is a question that needs to be addressed; therefore, my project is designed to examine the expression of p-p38(MAPK) in a mouse model of AD-related amyloidosis. The mouse model I used is the TgCRND8 mouse that expresses a variant of the human APP that contains polymorphisms that have been linked to AD. I chose to use immunohistochemistry and immunofluorescence to examine the distribution of the p-p38(MAPK) protein in both wildtype and TgCRND8 mouse cortex, and, more specifically, its distribution in relation to amyloid plaques. As it is difficult to draw any conclusions from the examination of the pathology at a single time point (or age), I chose to include mice at different ages; the age-dependent changes allowed me to determine more precisely the relation of p-p38(MAPK) to amyloid plaque formation. Rather than simply collecting qualitative data, which are also very difficult to interpret, I used stereology, which is a statistics-based sampling technique that allows for unbiased and accurate estimates of cells (including number, size and shape). Stereology allowed me to quantify and measure changes in p-p38(MAPK) distribution as a function of age and amyloid plaque deposition.

The use of specific markers and stains allowed me to identify different plaque types as well as the specific cell types that express p-p38(MAPK) in this context.

## 2. MATERIALS AND METHODS

### 2.1 Animal model

The APPSwe/Ind TgCRND8 mouse is a transgenic model of AD-related amyloidosis. These mice express a transgene incorporating both the Swedish mutation (K670N/M671L) and the Indiana mutation (V717F) in the human APP protein [134]. These authors have clearly demonstrated that expression of this transgene results in the production of Aβ and the aggregation of Aβ into plaques at a very early age (normally around 12-14 weeks). These mice were a gift from Dr. David Westaway at the Centre for Research Neurodegenerative Disease (University of Toronto, Toronto, ON, Canada). All procedures were performed in accordance with the Canadian Council on Animal Care Guidelines and were approved by the University of Saskatchewan Animal Care Committee (protocol# 20060070). Genotyping of all animal models was routinely performed by Paul Pennington, a member of the Cell Signalling Laboratory.

### 2.2 Antibodies

#### 2.2.1 p38(MAPK) antibodies

The p38(MAPK) protein was detected with a mouse monoclonal p38(MAPK) antibody (#9217) purchased from Cell Signalling Technology (Danvers, MA, USA). This antibody detects all of the isoforms of p38(MAPK) and does not cross-react with other MAPK kinases. The dilution ratio used for the immunohistochemistry and immunofluorescence was 1:100. The p-p38(MAPK) protein was detected using a rabbit polyclonal antibody (#9211) purchased from Cell Signalling Technology (Danvers, MA, USA). This antibody (used at a dilution of 1:100) recognizes the activated conformation of p38(MAPK), i.e. phosphorylated on threonine 180 and tyrosine 182.

#### 2.2.2 Plaque associated antibody

The mouse monoclonal anti-APP (6E10) antibody was used for detecting the amyloid deposits. This antibody is reactive to amino acid residues 1-16 of Aβ and was used at a concentration of 1:1000. This antibody was purchased from Covance (Princeton, NJ, USA).

### 2.2.3 Antibodies as cell markers

The mouse anti-neuronal nuclei (NeuN) monoclonal antibody (MAB337; clone A60) is a specific antibody for most neuronal cell types (exceptions include Purkinje cells, mitral valve cells and photoreceptor cells). The NeuN antibody was diluted at a ratio of 1:1000 and was obtained from Millipore (Billerica, MA, USA)

Astrocytes were detected using the mouse monoclonal anti-glial fibrillary acidic protein (GFAP) (G3893) at a dilution of 1:1000. The antibody was obtained from Sigma-Aldrich Ltd (St Louis, MO, USA)

Both of the mouse anti-Macrophage-1 (CD11b/CD18) (Mac-1)/anti-CD11b (MCA74G) and mouse anti-ectodermal dysplasia-1 (CD68) (ED-1)/anti-CD68 (MCA341R) antibodies were used for detecting microglia. The dilution used for these two antibodies was 1:1000. Both antibodies were obtained from Serotec (Raleigh, NC, USA).

All the antibodies mentioned above were diluted in PBS/0.3% Triton X-100 (PBS-TX). PBS (phosphate buffered saline) is a buffer solution widely used in biological research. This water-based salt solution maintains a constant pH and provides a condition with almost the same ion concentrations and osmolarity of human body. Triton X-100 is a non-ionic surfactant than can increase the permeability of the cell membrane and reduce solution surface tension during immunostaining. Making the antibody solution with PBS-TX can help to preserve the integrity and condition of the tissue sections, and also increase the quality of immunostaining. All primary antibodies were stored at -20°C.

## 2.3 Methods

### 2.3.1 Gelatin-coating slides

Pre-coating slides with gelatin helps affix tissue to the slides, and reduces the chance of a tissue sample being lost during processing. Slides were prepared as follows:

1) Melvin freed microscope slides were placed in slide racks.
2) The slides were soaked in fresh gelatin solution for ½ hour and dried overnight in at 60°C.

3) Repeat step 2.
4) Slides were stored in slide boxes at 4°C up to one month until use.

Preparation of fresh gelatin solution:

1) Add 2.5 g gelatin to 300 ml distilled water and heat to dissolve.
2) Cool to room temperature (RT).
3) Add chromium potassium sulfate [$CrK(SO_4)_2$].
4) Bring to volume (500 mL) with distilled water.

### 2.3.2 Perfusion and brain fixation

Mice were treated in accordance with the University Committee on Animal Care and Supply/Canadian Council on Animal Care guidelines. The 3-, 6- and 10-month TgCRND8 and wildtype mice were sacrificed and perfused by transcardial perfusion. The brains were removed and fixed for immunohistochemistry. Perfusion is a means of removing blood from the body and brain, which prevents antibodies from reacting non-specifically with molecules in the blood. Fixation crosslinks proteins in the tissue, thereby preventing proteins from being digested by enzymes. It can optimize preservation of cellular structures and antigens. In addition, it also prevents post-mortem decay and extrinsic damage by bacteria as well as increases the mechanical strength and stability of brain tissue. As a result, brains can also be stored for much longer prior to use.

1) Mice were anaesthetized by intraperitoneal injection of pentobarbital sodium (50 mg/kg) and closely monitored to make sure the animals were completely under the anesthetic.
2) Animals were immobilized on the operating table by taping the limbs. The thoracic cavity was then opened to expose the heart for transcardial perfusion.
3) A 10 ml syringe was filled with PBS and the left ventricle of the mouse's heart was cut open to allow for the PBS to drain from the circulatory system once it had perfused the brain (and the rest of the body). The heart was held in place with

forceps while the syringe was inserted into right atrium and PBS was pushed through the heart.

4) Once perfused, the head was detached and the skull was exposed. The cranial cavity was opened and the brain was removed and rinsed in PBS.
5) The brain was post-fixed in 4% paraformaldehyde (PFA) by immersion in approximately 5 ml of the solution for 24 h at 4°C.
6) The brain was then transferred into 30% sucrose, immersed in the solution for 48 h at 4°C, and frozen on dry ice.
7) The brain tissue was stored at -70°C until sectioned coronally.

Preparation of PBS:

1) Add 15.4 mg sodium hydrogen phosphate ($NaHPO_4$) and 67.3 mg sodium phosphate monobasic monohydrate ($NaH_2PO_4.H_2O$) into 2000 ml distilled water to make 2 M Phosphate Buffer (PB).
2) Add 18 mg sodium chloride and 100 ml 2 M PB in 1900 ml distilled water to make PBS.

Preparation of 4% PFA in 0.1M PB:

1) Mix 20 g PFA powder in 200 ml distilled water.
2) Heat to 60°C and add 2N NaOH drop-wise until solution is clear.
3) Bring volume up with distilled water to 250 ml and add 250 ml 0.2 M PB.

Preparation of 30% sucrose solution:

1) Make 130 mM Na Phosphate by mixing 72.9 ml 1M $Na_2HPO_4$ and 27.1 ml 1M $NaH_2PO_4$.
2) Dissolve 30 g sucrose in 100 ml of 130 mM Na Phosphate.

### 2.3.3 Brain sectioning

1) To avoid the activation of enzymes and to keep the brain in good condition, the temperature of the cryostat was kept at -20°C or lower. The fixed brain tissue was

transferred from -70°C to -20°C one day before being sectioned to bring the temperature of the tissue to that of the cryostat.

2) A 24-well plate was filled with PBS and placed on an ice pack.
3) The brain was taken from -20°C and placed in the cryostat chamber. The brain was then affixed to a metal base using tissue mounting medium. To ensure that the brain was firmly mounted in the mounting media, the procedure was completed on the cryobar set at -61°C.
4) The metal base was orientated on the specimen bar in a manner that allowed the brain to be sectioned coronally.
5) The section thickness of brain was 30 μm. This thickness was selected to allow for a) adequate penetration of the primary antibody into the tissue; and b) stereological quantification of the immunohistochemical markers used in the study.
6) The sectioned brain tissue was saved in the 24-well plate following the order of well number 1 to 24 in rotations.
7) The brain sections were transferred to another 24-well plate filled with PBS to rinse out any mounting medium still attached to the tissue sections, and then stored at 4°C overnight.
8) The brain sections were transferred in a 24-well plate filled with glycerol buffer and stored at 4°C until use.

### 2.3.4 Immunohistochemistry

Immunohistochemistry is based on the principle of the specific binding between antibodies and antigens (*e.g.* proteins) in the cells of the tissue section. All the immunohistochemical experiments in this project followed the 'indirect method', which involves the identification of the target protein by first binding the primary antibody to the target protein, and then detecting the antibody-protein complex with an enzyme-conjugated secondary antibody directed against the primary antibody. The immune complex can be visualized by conversion of a substrate (by the enzyme conjugate) to a visible product.

1) Brain sections were taken from the 4°C glycerol buffer and placed in an appropriate container (6-, 12-, or 24-well plate) filled with PBS.
2) The free-floating sections were washed 3 times in PBS (each wash = 30 min).
3) Sections were incubated for 30 min in 10 mM sodium citrate buffer at 70°C for antigen retrieval and the sections were cooled (RT, 30 min).
4) Sections were washed 3 times in PBS (each wash = 15 min).
5) Sections were immersed in 0.2% $H_2O_2$ for 30 min to inhibit endogenous peroxidase activity following three 15 min washes in PBS.
6) Sections were incubated (RT, 1.5 h) in 5% normal serum in PBS-TX to block the non-specific binding of primary and secondary antibodies.
7) Sections were then incubated for 72 h at 4°C and 2 h at RT in PBS-TX with the primary antibody.
8) Sections were washed 3 times in PBS (each wash = 30 min).
9) Sections were blocked with 2.5% normal serum before adding the secondary antibody in PBS-TX for 1h.
10) Sections were incubated with the secondary antibody (RT, 1.5 h) in PBS-TX followed by three 20 min PBS washes.
11) Sections were incubated with the avidin-biotin complex solution (ABC kits) (Vector Laboratories, Inc., Burlington, ON, Canada) for 1 h following 3 times 15 min PBS washes.
12) Sections were processed by the 3,3′-diaminobenzidine (DAB) staining method for 15-30 min for colorimetric visualization and then transferred into PBS.
13) Sections were mounted on gelatin-coated slides and dried overnight.
14) Mounted sections were immersed in ascending ethanol concentrations for dehydration, and then placed in xylene for clearing and dissolving ethanol.
15) Slides with sections were cover-slipped with Permount Mounting Media (Sigma Aldrich Ltd.) and prepared for microscopy.

Preparation of 0.2% $H_2O_2$ in PBS:

1) Add 100 µl $H_2O_2$ to 900 µl distilled water to make 30% $H_2O_2$.
2) Add 332.75 µl of 30% $H_2O_2$ to 50 ml PBS to make 0.2% $H_2O_2$.

Preparation of PBS/0.3% Triton X-100 (PBS-TX):

1) Dilute 5 ml Triton X-100 with PBS (to a volume of 50 ml) to make 10% Triton.
2) Add 1.5 ml 10% Triton to 48.5 ml of PBS to make 0.3% Triton.

Preparation of DAB staining reagent:

1) Dissolve 500 mg DAB powder in 190 ml distilled water.
2) Add 10 ml 2 M PBS and then add 1.8 mg NaCl.
3) Aliquot the DAB staining reagent into 50 ml falcon tubes (each tube = 10 ml) and freeze until use.
4) To use DAB, thaw the frozen aliquot and then add 40 ml PBS and 50 µl of 30% $H_2O_2$.

### 2.3.5 Immunofluorescence

Immunofluorescence is based on the same principle as immunohistochemistry. However, the secondary antibodies are already labeled with a colorimetric indicator (i.e., a fluorochrome). This means that once the primary antibody detects the target protein and forms an immune complex with the secondary antibody, the interaction will be visualized without any further processing. Antibodies used for immunofluorescence, e.g. anti-total p38, anti-p-p38, 6E10, NeuN, GFAP, Mac-1 and ED-1, were described in the 'Antibodies' section above.

Procedure for immunofluorescence:

1) Brain sections were taken from 4°C glycerol buffer and placed in the appropriate plates containing PBS.
2) Free-floating sections were washed 3 times in PBS for 30 min and left overnight at 4°C.
3) Following 3 washes in PBS (each wash = 20 min, RT), sections were incubated for 30 min in 10 mM sodium citrate buffer at 70°C for antigen retrieval. The sections were then allowed to cool (RT, 30 min).
4) Sections were washed 3 times in PBS for 15 min.

5) Sections were blocked (1.5 h, RT) in 5% normal serum in PBS-TX.
6) Sections were then incubated for 72 h at 4°C and 2 h at RT in PBS-TX with two primary antibodies (so as to target two different proteins concurrently).
7) Sections were washed 3 times in PBS for 30 min.
8) Sections were blocked in 2.5% normal serum in PBS-TX for (RT, 1 h) before adding the secondary antibody.
9) Sections were incubated 1.5 h (RT) with the appropriate two fluorescent secondary antibodies raised against the two primary antibodies in PBS-TX (used in point 6, above).
10) Sections were washed 3 times in PBS for 20 min and mounted on gelatin-coated slides.
11) Prolong Gold Fluorescent Mounting Media (Invitrogen #P36930) was added to the sections and these were then covered with a coverslip and prepared for confocal microscopy.

Fluorescence secondary antibodies include: Alexa Fluor 488 donkey anti-mouse, 488 donkey anti-rabbit, 594 donkey anti-rabbit, 555 goat anti-mouse, 555 goat anti-rabbit (all from Invitrogen).

### 2.3.6 Staining methods

Both of the Thioflavin-S staining and Nissl staining are reported as reliable markers of the central core of 'dense-core' plaques. Therefore, these two staining methods were used in this project to detect the cores.

#### 2.3.6.1 Thioflavin-S staining

1) Sections were transferred from glycerol buffer to PBS and washed 3 times in PBS for 30 min
2) Sections were mounted on gelatin-coated slides and were allowed to dry.
3) Slides with sections were placed in the slide racks.
4) The slide racks were immersed in a glass trough filled with 1% Thioflavin-S for 5 to 10 min.

5) The slides were taken from the Thioflavin-S solution and placed in an empty glass trough. The slides were rinsed in running water for 2 min (Running water should be added gently along a corner of the trough to avoid sections being flushed off of the slides).
6) Slides were covered in 70% ethanol for 5 min (twice).
7) Sections were covered with Prolong Gold Fluorescent Mounting Media (as above).

1% Thioflavin-S solution:

10 mg Thioflavin-S powder in 1 ml distilled water.

**2.3.6.2 Nissl (Thionin) staining**

1) Sections were transferred from glycerol buffer to PBS and washed 3 times in PBS for 30 min each.
2) Sections were mounted on gelatin-coated slides and allowed to dry before use.
3) Slides with sections were placed in the slide racks.
4) The slide racks were immersed in glass trough filled with 0.2% Thionin solution for 5 to 10 min.
5) Slides were rinsed quickly in distilled water.
6) The slide racks were placed in 50%, 70%, 95% and 100% ethanol for 15 min respectively.
7) Sections were cleared in xylene for 15 min (twice).
8) Slides were cover-slipped with Permount Mounting Media.

0.2% Thionin solution:

2 mg Thionin powder in 1 ml distilled water.

**2.3.7 Stereological quantitative analysis**

Stereology is a sampling method that can be used to quantify and measure cell number, type, size; regional volume; area fraction, etc. in a three-dimensional space. Compared with traditional counting methods, stereology is more precise and unbiased. In

this project, the number of p-p38(MAPK) immunoreactive (IR) cells in the sensorimotor cortex of wildtype and TgCRND8 mice was quantified using StereoInvestigator software (at 40X magnification). Sections from the wildtype and TgCRND8 mouse brains were processed for p-p38(MAPK) DAB immunohistochemistry. p-p38-IR cells appeared as brown (because of the DAB).

The optimal counting frame size to be used for stereology was determined through a preliminary population estimate, which resulted in a 100 $\mu m^2$ counting frame distributed in a 150 $\mu m^2$ counting grid (Figure 5). The average section thickness was 14 μm. Therefore, p-p38(MAPK)-IR cells were counted through a depth of 12 μm, leaving a 2 μm guard zone at the top of the section.

The StereoInvestigator software complementing a BX-51 fluorescence microscope system (Olympus Canada; Markham, ON, Canada) was used as follows:

1) Sections were placed on the microscope stage and the region of interest (the sensorimotor cortex) was identified using the 4X objective.
2) A 'live' image of the brain region was viewed on the computer screen.
3) Information regarding the number of sections to be counted, the thickness of the cut sections, and the section evaluation interval was entered into the software.
4) A box was drawn to outline the sensorimotor cortex in each brain section.
5) The size of the counting grid (Figure 5) was entered into the software. A "counting frame" (i.e., a "sampling box") was placed within each counting grid automatically by the software.
6) The cell numbers were counted in the counting frame under 40X magnification. For each counting frame, cells were first counted in the two-dimensional plane at the top of a section (Shown as the top picture in Figure 5). When cells touched the border of the counting frame, only the cells on the green border were counted, whereas cells which touched the red border of the counting frame were not counted. Given that the diameter of the p-p38(MAPK) cells is less than the thickness of section (shown as the bottom picture in Figure 5), there was more than one layer of p-p38(MAPK) cells in a section. Therefore, after the counting of the top layer was completed, the counting frame was moved through the Z-axis to

the next layer and cells were counted in this layer by the same way. When all cells in all layers were counted from the top to bottom of the section, the cell counting in this counting frame was finished. However, cells were not counted if they came into focus within the 2 μm 'guard zone' at the top of the tissue.

7) After all the cells in all the counting frames were counted, the mean cell count per sampling box (per unit area) was then calculated.

Amyloid plaques were identified by Thioflavin-S (detects the fibrillar conformation of amyloid) and/or 6E10 (the anti-APP/Aβ antibody). It became apparent that a clustering of three or more p-p38(MAPK)-IR cells was a reliable marker of Aβ plaques, and thus these three or more cells that were in direct contact with a plaque were counted as 'plaque-associated p-p38 (MAPK)-IR cells'. In contrast, p-p38(MAPK)-IR cells were counted as 'parenchymal' cells if they were distributed throughout the parenchyma and were not adjacent to two or more other p-p38(MAPK)-IR cells or to a plaque. The density of 'plaque-associated' as well as 'parenchymal' p-p38(MAPK)-IR cells were estimated across all the six layers of the cortex on six sections to bring the coefficient of error in sampling variance to <0.05.

### 2.3.8 Confocal microscopy

The distribution of p-p38(MAPK)-IR cells around 6E10-positive 'diffuse' plaques was observed using the 40X air objective and a BX71 Olympus confocal microscope (and Fluoview SV500 software). Double-labeled images of the p-p38(MAPK)-IR cells with different cell markers (e.g. NeuN, GFAP, Mac-1 and ED-1) were obtained under the 60X oil immersion lens. Double-immunofluorescence for p-p38(MAPK) and total p38(MAPK) was captured using the 100X oil immersion lens. The main procedure of taking pictures under confocal microscopy was as follows:

1) The region of interest was selected.
2) The 'live view' image was captured and displayed in the Fluoview software.
3) The brightness and contrast of the live image were optimized.
4) The coordinates for the top and bottom of the section were identified using the software and set up in the Z-axis.

5) The scanning interval through the thickness of section was set up (*e.g.* if the section is 10 μm thick and the interval is set up as 1 μm between each scanning, 11 layers of the section will be scanned and captured by the software).
6) Scanning was started under the 'XYZ' mode, in which section will be scanned from the top to bottom along the Z-axis.
7) The two transmission channels (from the Ar and He lasers) were captured simultaneously and filtered by 8 Kalman low-speed scans.

### 2.3.9 Statistics

All statistics were performed using Graphpad Prism (v3.01), unless stated otherwise. Significance (set at $p<0.05$) was assessed by one-way or two-way ANOVA with post-hoc analysis based on Bonferroni's Multiple Comparison Test. The Pearson product-moment correlation coefficient was used to measure the strength of the linear relationship between factors, e.g. the number of plaque-associated p-p38(MAPK)-IR cells and the core size [i.e. absolute core size or core size as a proportion of the size of the plaque within which it is located]. The stereological statistical sampling protocol is described in the 'Stereological quantitative analysis' section above and was performed using the StereoInvestigator software (MicroBright-Field, Inc.). Data are represented as mean ± SEM, and P-values are provided as summary statistics.

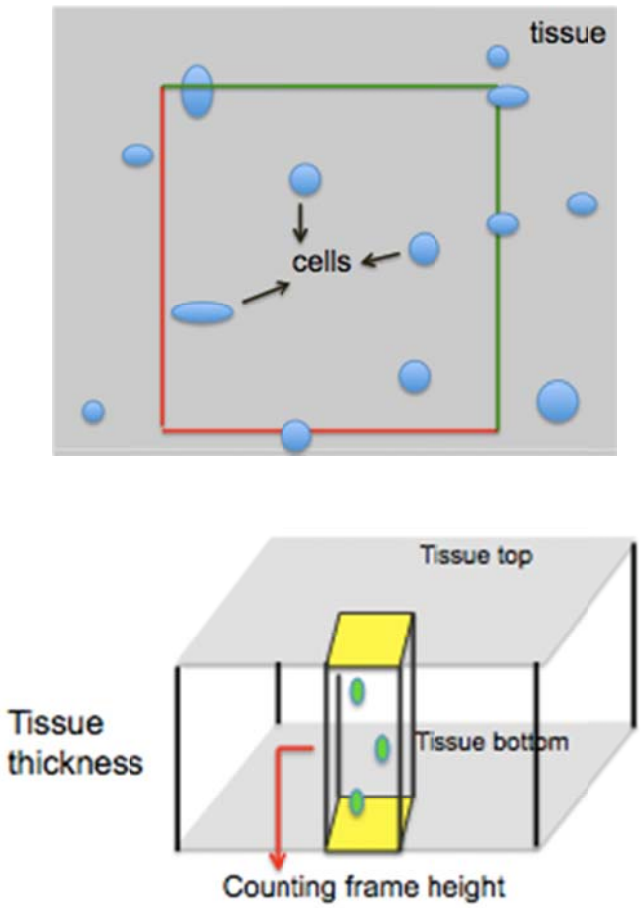


**Figure 5.** *(top)* Schematic of counting frame in a tissue section. *(bottom)* Section including multiple layers of cells through its thickness. (image adapted from http://www.uhnresearch.ca/facilities/wcif/PDF/StereoInvestigator.pdf).

## 3. RESULTS

### 3.1 Fibrillar and non-fibrillar Aβ increase with age in the sensorimotor cortex of TgCRND8 mice.

To confirm the TgCRND8 mouse as an aggressive model of AD-related amyloidosis, the progression of amyloid plaque deposition in 3-, 6- and 10-month TgCRND8 mice was assessed by both 6E10 (anti-APP) immunofluorescence and Thioflavin-S staining (Figure 6). A 10-month-old wildtype mouse was included as a control. 6E10 immunoreactivity as well as Thioflavin-S-positive plaques were detected in young animals (confirming the aggressive nature of the transgene) and appeared to increase in an age-dependent manner in the sensorimotor cortex in the TgCRND8 mouse sections. Plaques were not detected in the 10-month-old wildtype mouse. Two types of plaque, 'dense-core' and 'diffuse' plaques were observed. In 'dense-core' plaques, a solid central core showed stronger 6E10 immunoreactivity (IR) than the peripheral part of the plaque, which surrounded the central core as a halo (Figure 7). However, the pattern of 6E10-IR and Thioflavin S staining within 'diffuse' plaques was quite distinct from the 'dense-core' plaques. Diffuse plaques were characterized by a punctate 6E10-IR that was evenly distributed over the entire plaque, without any distinct 6E10-IR or Thioflavin-S staining in the center of the plaque. Merging of Thioflavin-S staining and 6E10-IR from the same 'dense-core' plaque showed a complete co-localization, confirming the identity the 'dense-core' plaque. Furthermore, Thioflavin-S selectively stained the 'dense-core' plaques, providing us with a quick means to distinguish the two different kinds of plaques.

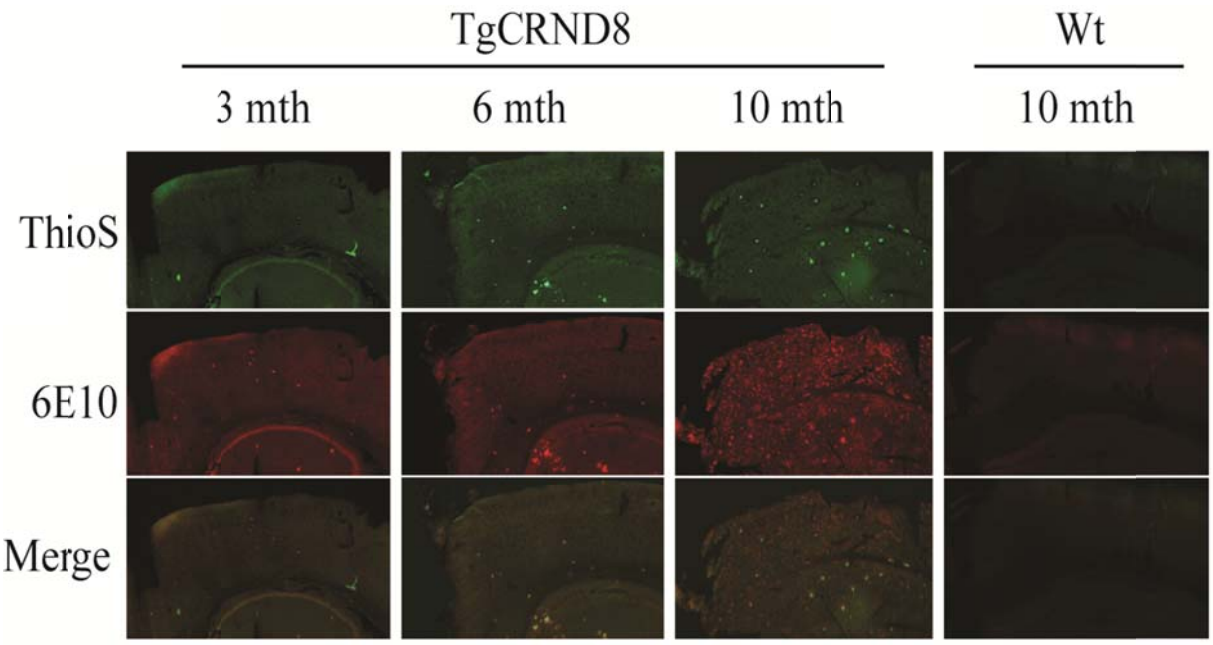


**Figure 6. Photomicrographs of progressive amyloid plaque deposition in sagittal sections of sensorimotor cortex.** Thioflavin-S staining (ThioS: green) and 6E10 immunofluorescence (identifies human APP: red) were applied to sections of 3-, 6- and 10-month (mth) TgCRND8 mice. Amyloid plaque deposition is shown as the brightly punctuate dots in the sensorimotor cortex of TgCRND8 mice. The age-dependent increase in plaque deposition is revealed by both Thioflavin-S staining and 6E10 immunofluorescence. The fibrillar conformation of Aβ is identified specifically by Thioflavin-S staining, whereas 6E10 immunofluorescence detects both fibrillar and non-fibrillar Aβ species. A section from 10-month-old wildtype mouse in which Thioflavin-S and 6E10 immunoreactivity is clearly not detected is included for comparison. The 'Merge' figures demonstrate the overlap in the distribution of the ThioS staining and 6E10-immunoreactivity. Scale bar, 400 μm.

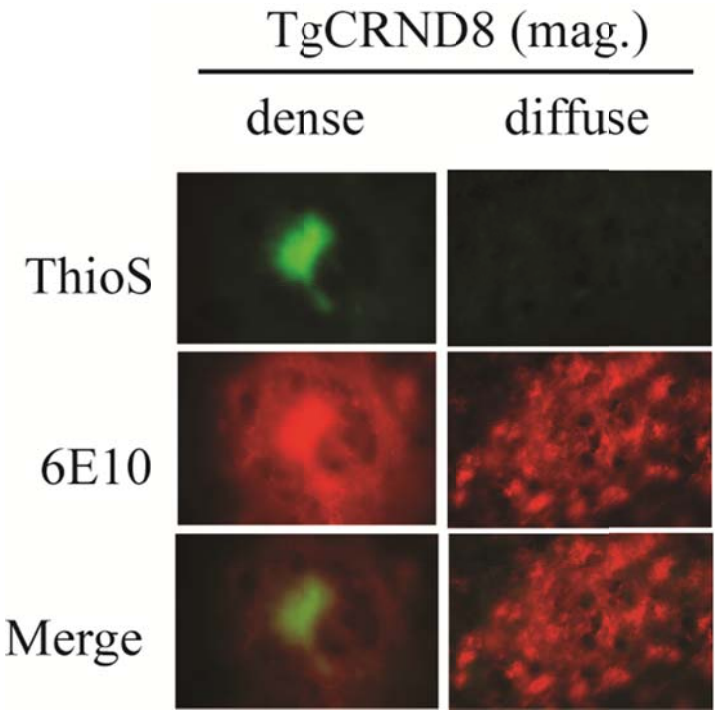


**Figure 7. Two types of plaque are identified in the TgCRND8 sensorimotor cortex.** Thioflavin-S staining (ThioS: green) and 6E10 (anti-APP) immunofluorescence (red) of amyloid plaques is revealed (100X oil objective). Two types of plaques, 'dense-core' *(left column)* and 'diffuse' *(right column),* show distinct patterns of 6E10 immunofluorescence. Thioflavin-S staining can recognize the central core of the 'dense-core' plaque but does not stain the 'diffuse' plaque. In the dense core plaque, the thioflavin-S-positive core completely co-localized (in the 'Merge' panel, bottom left) with the core detected by the 6E10 immunofluorescence. Scale bar, 10 μm.

### 3.2 Distribution of p-p38(MAPK) immunoreactivity in sensorimotor cortex of wildtype and TgCRND8 animals.

Double-labeled immunofluorescence was performed with anti-p-p38(MAPK) and anti-p38(MAPK) [recognizes total p38(MAPK)] in sections from wildtype and TgCRND8 animals. As expected, the p-p38(MAPK)-IR cells were also p38(MAPK)-IR (Fig 8). Although the p-p38(MAPK)-IR was predominately localized in the nucleus, whereas the p38(MAPK)-IR was primarily observed in the cytoplasm, this is expected as the activated form of p38(MAPK) does translocate to various subcellular compartments. Co-localization of the two signals was evident in the cell's processes (Figure 8).

Brain sections from 3-, 6- and 10 month wildtype and TgCRND8 animals were stained by DAB-immunohistochemistry with the anti-p-p38(MAPK) antibody. In both the wildtype and TgCRND8 mouse cortex, the same pattern of equidistantly distributed p-p38(MAPK)-IR cells were detected throughout the parenchyma of the sensorimotor cortex at 3-, 6- and 10-months (Figure 9). In addition, a higher density of p-p38(MAPK)-IR cells was observed in the vicinity of patches [amyloid plaques?] in TgCRND8 mice. In accordance with the results revealed by the 6E10 immunofluorescence and Thioflavin-S staining (Figure 6), the patches increased with age in TgCRND8 mice and there were no 'patches/plaques' found in wildtype mice. A section without the primary antibody [anti-p-p38(MAPK)] was included as a control and clearly shows a lack of p-p38(MAPK) signal. These data (Figure 9) confirmed the specificity of the anti-p-p38(MAPK) antibody and suggested that p-p38(MAPK)-IR cells are also associated with amyloid plaques.

An association between p-p38(MAPK) and amyloid plaques was suggested, yet it was unclear one or both types of plaques identified in Figure 6 were associated with p-p38(MAPK)-IR. The DAB-immunohistochemistry sections were then stained using Thioflavin-S and thionin/Nissl stain (stains nucleic acids (DNA/RNA) and is useful for viewing cells). The thionin staining of the central core of the plaque was paralleled by staining for Thioflavin-S. Some of the plaques showed neither Thioflavin-S nor thionin staining, but did show 6E10-IR. Interestingly, p-p38(MAPK)-IR cells were observed in clusters that surrounded both types of plaques. This demonstrated that p-p38(MAPK)-IR cells were associated with both 'dense-core' and 'diffuse' plaques. In addition, several vasculature-associated p-p38(MAPK)-IR cells were also detected (Figure 10).

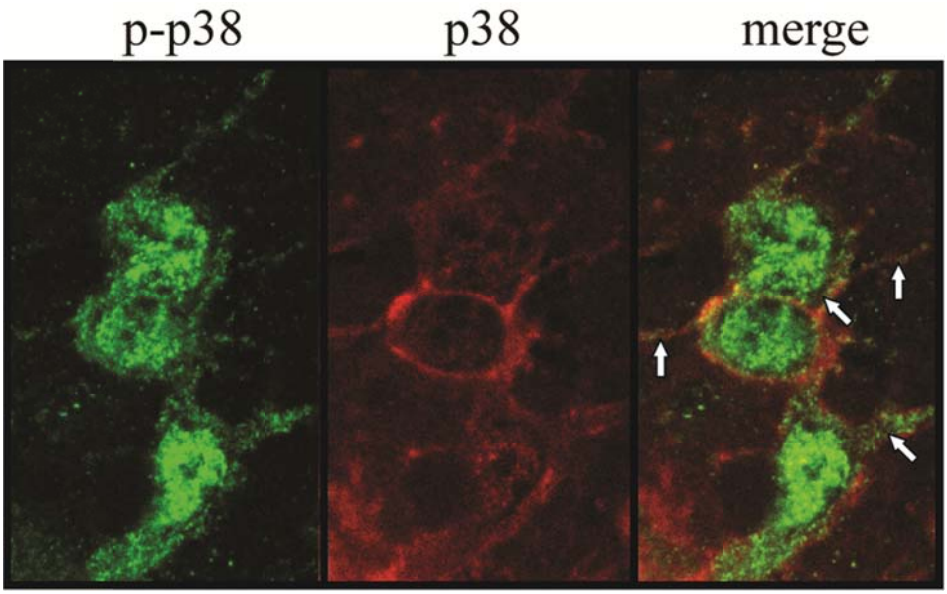


**Figure 8. Anti-p-p38(MAPK) and anti-p38(MAPK) recognize the same cells in mouse cortex.** The specificity of the anti-p-p38(MAPK) (p-p38) and anti-p38(MAPK) (p38) antibodies was tested by comparing the signal patterns within a given cell (using fluorescence microscopy). Although the p-p38(MAPK) (green) signal is predominately in the nucleus and the p38(MAPK) (red) is predominately in the cytoplasm, co-localization of both signals can be observed in cell membranes and processes (indicated with the arrows). Scale bar, 5 μm.

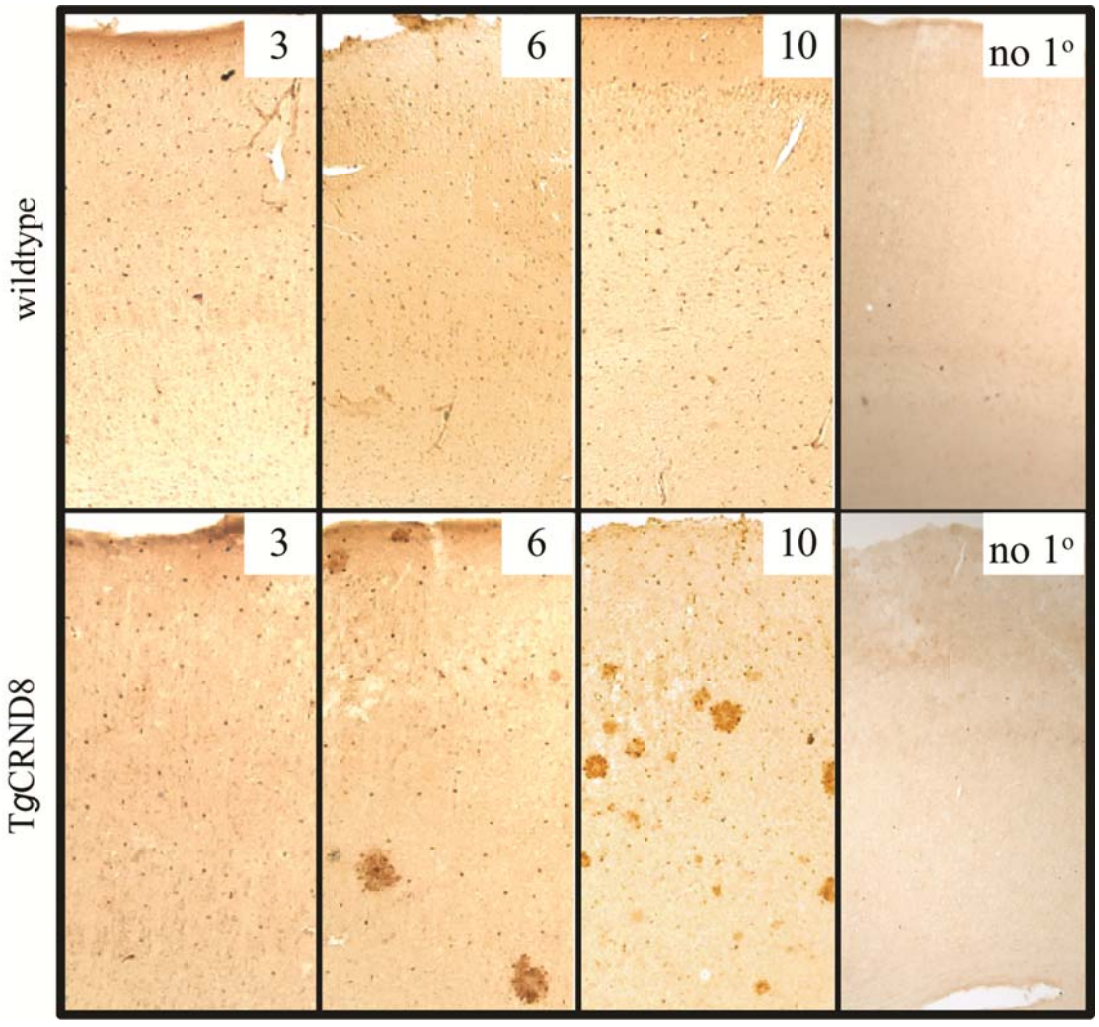
wildtype
TgCRND8
3
6
10
no 1°
3
6
10
no 1°

(Previous page)

---

**Figure 9. The distribution of p-p38(MAPK)-IR cells in sensorimotor cortex of wildtype and TgCRND8 mice.** DAB-immunohistochemistry was used to examine the distribution of p-p38(MAPK) immunoreactivity in sections of 3-, 6- and 10-month wildtype and TgCRND8 animals. Parenchymal p-p38(MAPK)-IR cells are observed as the black dots that are evenly distributed in the parenchyma of wildtype as well as TgCRND8 mice cortex at all ages. Meanwhile, DAB-positive patches (subsequently identified as amyloid plaques) increase in an age-dependent manner as does the number of p-p38(MAPK)-IR cells in the vicinity of these patches. A section without the primary antibody (‘no 1°’) is included for comparison. Scale bar, 100 μm.

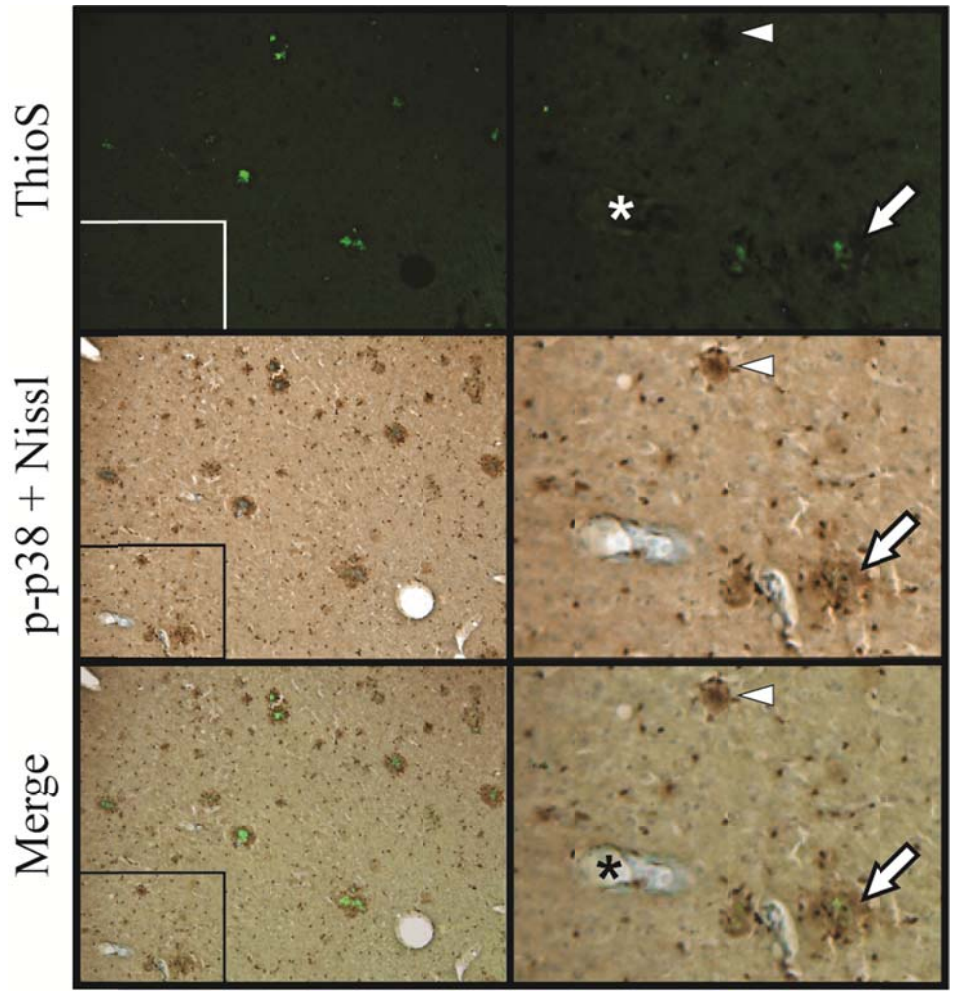


**Figure 10. p-p38(MAPK)-IR cells surround both 'dense-core' and 'diffuse' plaques.** A section from a 10-month-old TgCRND8 mouse was triple labeled with Thioflavin-S staining (green, top panel), thionin/Nissl staining (purple, middle panel) and DAB-immunohistochemistry (brown, middle panel) for p-p38(MAPK)-IR. The panels on the right are magnifications of the boxed area within the corresponding panels on the left. A Thioflavin-S- and thionin-positive 'dense core' plaque is indicated by the arrow, whereas the arrowhead indicates a Thioflavin-S- and thionin/Nissl-negative 'diffuse' plaque. DAB-immunohistochemistry revealed that p-p38(MAPK)-IR cells localize to both types of plaques. The asterisk indicates vasculature-associated p-p38(MAPK)-IR cells. Scale bar, 125 μm.

### 3.3 Quantification of p-p38(MAPK)-IR cells in sensorimotor cortex of TgCRND8 mice

It was observed that p-p38(MAPK)-IR cells were expressed in the sensorimotor cortex of both wildtype and TgCRND8 animals at all three ages. As well, a higher density of p-p38(MAPK)-IR cells was observed in the vicinity of amyloid plaques. However, the reason for the localization of p-p38(MAPK) to amyloid plaques could not be defined until aspects of amyloid plaques and p-p38(MAPK)-IR cells were quantified.

The mean number of cells (MCC) per unit volume of p-p38(MAPK)-IR cells in the sensorimotor cortex of 3-, 6- and 10-month wildtype and TgCRND8 animals were obtained by stereological sampling and compared using two-way ANOVA (Figure 11). An increased total MCC was observed in the TgCRND8 mice when compared to age-matched wildtype animals, indicating that genotype accounted for the increase in total MCC. As well, age exerted an effect. This was supported statistically: e.g. changes in the total MCC were dependent on both genotype ($F_{1, 12} = 89.8$, $P < 0.0001$) and age ($F_{2, 12} = 16.97$, $P = 0.0003$). Examining the data for associations with specific cell populations (e.g. splitting the 'total' MCC into 'parenchymal' MCC and 'plaque-associated' MCC) revealed no change in parenchymal MCC with genotype ($F_{1, 12} = 0.0990$, $P = 0.7584$) and a modest change with age ($F_{2, 12} = 5.517$, $P = 0.02$). In contrast, plaque-associated MCC showed a significant effect for both genotype ($F_{1, 12} = 184.2$, $P < 0.0001$) and age ($F_{2, 12} = 36.35$, $P < 0.0001$). The genotype and age-related increases in total MCC was exclusively due to the increase in plaque-associated p-p38(MAPK)-IR MCC (Figure 11A).

3-, 6- and 10-month TgCRND8 mice were then used to quantify the density of plaques in sensorimotor cortex. The number of both cortical 'dense-core' and 'diffuse' plaques was estimated in the same cortical volume. Both plaque types increased with age, although the age-dependent increase was more remarkable for the 'dense-core' plaques ($F_{2, 6} = 44.68$, $P = 0.0002$) than 'diffuse' plaques ($F_{2, 6} = 20.85$, $P = 0.002$). In addition, the increased density of amyloid plaques, especially the 'dense-core' plaque (by virtue of greater availability than that of diffuse plaques: Figure 11B), could be the type of plaque preferentially targeted by the 'plaque-associated p-p38(MAPK)-IR' cells in the sensorimotor cortex of TgCRND8 mice. This notion was examined next.

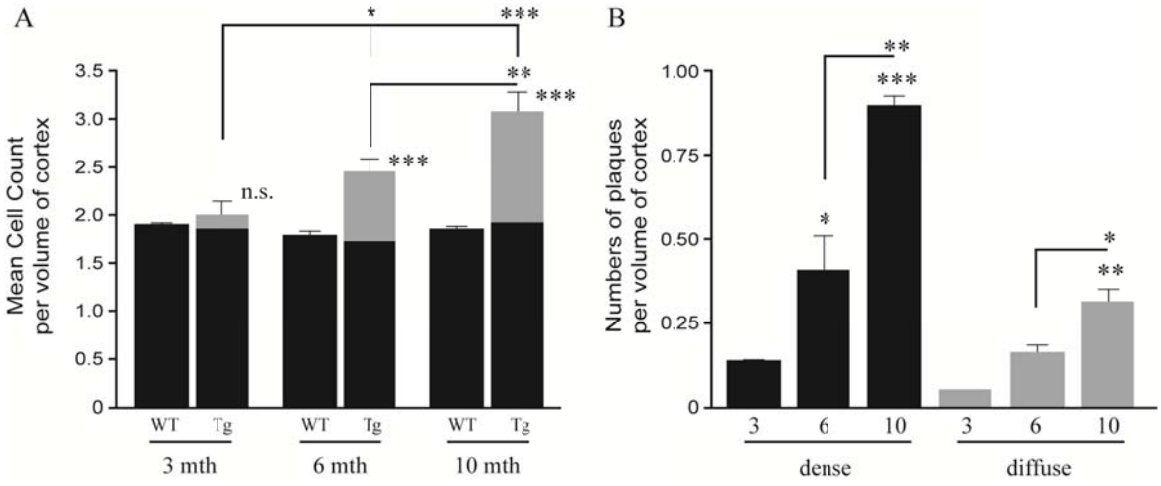


**Figure 11. Quantification of mean cell count and numbers of plaques per cortex volume.** Sections from 3-, 6- and 10-month wildtype and TgCRND8 mice, which were probed for p-p38(MAPK)-IR cells using DAB-immunohistochemistry, were quantified using stereological sampling. (A) p-p38(MAPK)-IR cells were categorized as parenchymal (black bars) and plaque-associated (grey bars) p-p38(MAPK)-IR cells. Total mean cell count (MCC), parenchymal MCC and plaque-associated MCC were quantified individually. The density (number of cells per volume of cortex) of parenchymal p-p38(MAPK)-IR cells remains constant with age, whereas plaque-associated p-p38(MAPK)-IR cells increase with age, indicating that the age-dependent increase in the density of the total p-p38(MAPK)-IR cells is exclusively associated with the plaque-associated p-p38(MAPK)-IR cells. (B) The density of both 'dense-core' plaques and 'diffuse' plaques increase with age, but the increase of 'dense-core' plaques is greater. *n* = 3-4 animals; **P* <0.05; ***P* < 0.01; ****P* < 0.001; *n.s.*, not significant.

Examinations were performed in the 3-, 6- and 10-month TgCRND8 mice. The size of individual 'dense-core' plaques significantly increased with age ($F_{2, 234} = 12.17$, $P < 0.0001$); however, the size of individual 'diffuse' plaques was not significantly different across age groups ($F_{2, 91} = 1.561$, $P = 0.2155$) (Figure 12A). The number of p-p38(MAPK)-IR cells per 'diffuse' plaque also remained unchanged with age ($F_{2,91} = 0.6351$, $P = 0.5322$). Interestingly, compared with the 3-month-old TgCRND8 mice, the number of p-p38(MAPK)-IR cells located in individual 'dense-core' plaques increased in the 6-month-old TgCRND8 mice ($F_{2,234} = 9.513$, $P < 0.0001$). However, the increase was no longer significant or even showed a slight decrease in the 10-month-old TgCRND8 mice (Figure 12B). The mean number of p-p38(MAPK)-IR cells per plaque area and per core area were quantified, and the number of 'dense-core' plaque-associated p-p38(MAPK)-IR cells decreased as a function of the plaque size ($F_{2,234} = 10.92$, $P < 0.0001$) (Figure 12C) and core size with age ($F_{2,234} = 70.16$, $P < 0.0001$) (Figure 12D). In addition to the quantification of the mean number of 'dense-core' plaque-associated p-p38(MAPK)-IR cells, the number of 'diffuse' plaque-associated p-p38(MAPK)-IR cells was not significantly changed ($F_{2,91} = 0.7643$, $P = 0.4686$) (Figure 12C). Furthermore, the average size of Thioflavin-S positive cores increasing with age was observed when the mean number of p-p38(MAPK)-IR cells per core area was examined ($F_{2,234} = 19.52$, $P < 0.0001$) (Figure 12D). These data suggest that the growth of 'dense-core' plaques will slow down with age, but the fibrillar conformation of the Aβ, Thioflavin-S positive core itself will continue to develop with age; and that the core development is inversely correlated with the number of plaque-associated p-p-38(MAPK)-IR cells.

The graphs and explanations for all the quantification and analyses, especially for the 'dense-core' plaque-associated p-p38(MAPK)-IR cells, could be better understood with an example of the analyses. One such example is given on the next page.

**Table 1. The example of stereological quantification and analyses**

| Age of TgCRND8 mice | Plaque ① number /cortex volume | Cell ② number /plaque | Cell number /cortex volume | Plaque size ($\mu m^2$) | Cell number /plaque area | Core size ($\mu m^2$) | Cell number / core area |
|---|---|---|---|---|---|---|---|
| 3-month | 1 | 2 | 2 | 1 | 2 | 1 | 2 |
| 6-month | 2 | 4 | 8 | 3 | 1.33 | 2.25 | 1.78 |
| 10-month | 5 | 3 | 15 | 3.25 | 0.92 | 3 | 1 |

①: The 'plaque' in the table represents 'dense-core' plaque.
②: The 'cell' in the table represents 'dense-core' plaque-associated p-p38(MAPK)-IR cells.

In this table, the number of 'dense-core' plaque-associated p-p38(MAPK)-IR cells per volume of cortex, the number of 'dense-core' plaques per volume of cortex, the 'dense-core' plaque size and the Thioflavin-S positive core size all increase with age. This is demonstrated in Figures 11A, 11B, 12A and 12D, respectively. The number of 'dense-core' plaque-associated p-p38(MAPK)-IR cells per plaque increases in 6-month-old TgCRND8 mice and then shows a decrease in 10-month-old mice, matching with Figure 12B. Interestingly, although all these are increased over the 3-month samples, the calculation of the number of 'dense-core' plaque-associated p-p38(MAPK)-IR cells per plaque area and per core area are decreased, supporting the graphs/data in Figures 12C and 12D.

### 3.4 The correlation between p-p38(MAPK)-IR cell density differs with absolute and proportional core size

The number of p-p38(MAPK)-IR cells was clearly associated with core development in 'dense-core' plaques. Therefore, it was necessary to determine whether there was an actual correlation (using Pearson's correlation) between the mean number of p-p-38(MAPK)-IR cells per 'dense-core' plaque and core size. The proportional core size

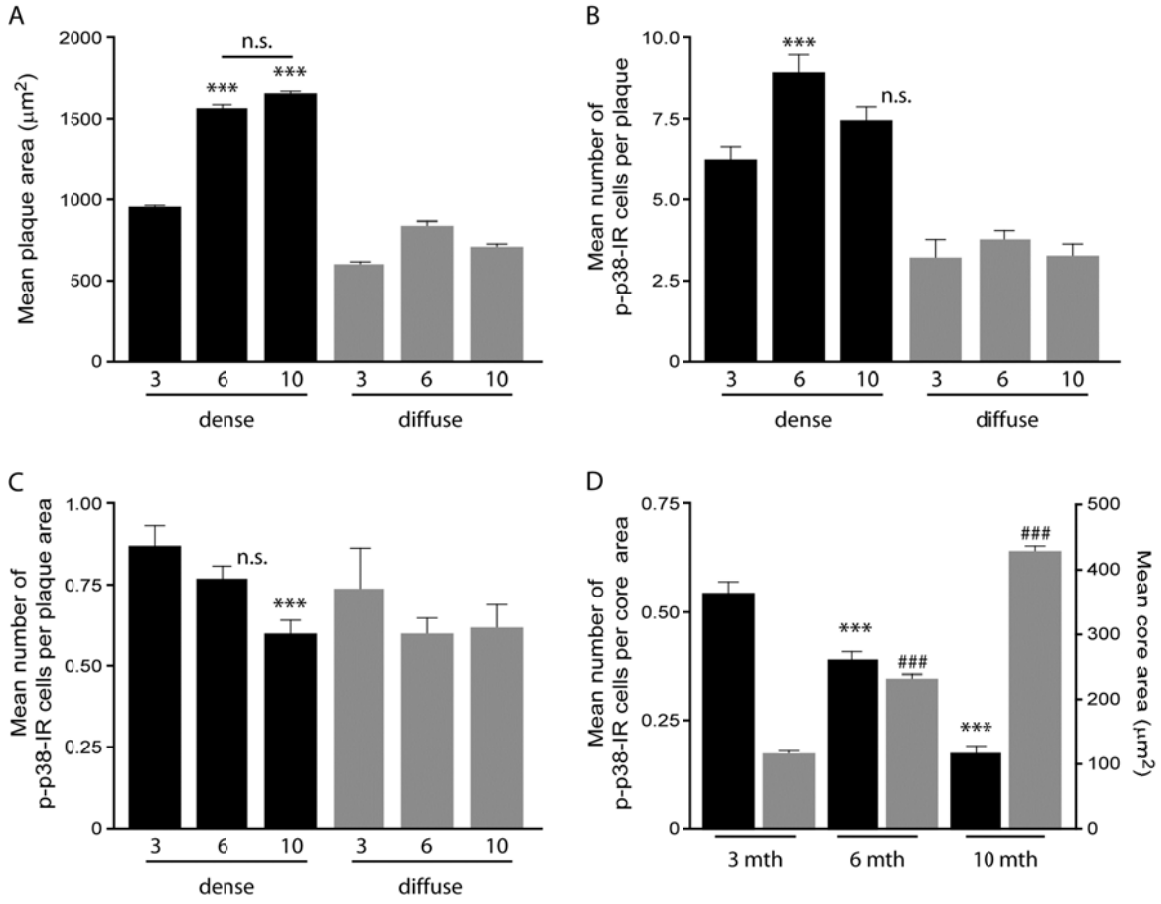
A
Mean plaque area (μm²)
2000
1500
1000
500
0
n.s.
***
***
3
6
10
3
6
10
dense
diffuse
B
Mean number of p-p38-IR cells per plaque
10.0
7.5
5.0
2.5
0
***
n.s.
3
6
10
3
6
10
dense
diffuse
C
Mean number of p-p38-IR cells per plaque area
1.00
0.75
0.50
0.25
0
n.s.
***
3
6
10
3
6
10
dense
diffuse
D
Mean number of p-p38-IR cells per core area
0.75
0.50
0.25
0
Mean core area (μm²)
500
400
300
200
100
0
***
###
***
###
3 mth
6 mth
10 mth

(Previous page)

---

**Figure 12. p-p38(MAPK)-IR cells are associated primarily with dense-core plaques.** Sections from 3-, 6- and 10-month TgCRND8 mice were used for the quantification. (A) The average size of 'dense-core' plaques increases with age, whereas the size of 'diffuse' plaques modestly changes with age. (B) The mean number of p-p38(MAPK)-IR cells per 'dense-core' plaque increases in 6- vs. 3-month-old mice, but this effect of age is no longer significant in the 10-month-old mice. The number of p-p38(MAPK)-IR cells per 'diffuse' plaque basically remains unchanged with age. (C) The number of p-p38(MAPK)-IR cells associated with 'dense-core' plaques decreases as a function of the plaque size with age, but there is no effect associated with 'diffuse' plaques. (D) The mean number of p-p38(MAPK)-IR cells per volume of core decreases (black bars), while the size of dense cores increases with age (grey bars). $n$ = 3-4 animals; $^{*}P < 0.05$; $^{**}P < 0.01$; $^{***}P$ ($^{###}P$) $< 0.001$; *n.s.*, not significant.

was defined as the percentage of the total 'dense-core' plaque area that is occupied by the Thioflavin-S positive core. The absolute core size and absolute 'dense-core' plaque size were measured in the sensorimotor cortex of all the three ages of TgCRND8 mice, and the proportional core size was then calculated using the values of absolute core size and absolute plaque size. The linear relation between the mean number of p-p38(MAPK)-IR cells and absolute core size revealed a positive correlation between these two parameters, with the strength of the correlation increasing with age [the age of the animal increases from panels A to B to C] (Figure 13). Conversely, a negative correlation between the mean number of p-p38(MAPK)-IR cells and proportional core size was observed, but the correlation was lost as a function of age [the age of the animal increases from panels D to E to F]. Statistical summaries are included in the actual figure.

### 3.5 The core of 'dense-core' plaque expands along the aspect that is devoid of p-p38(MAPK)-IR cells

It was initially observed that DAB-immunohistochemistry could stain patches that were subsequently identified as plaques (Figure 9) and that thionin staining could identify Thioflavin-S-positive deposits (Figure 10). Using these basic principles, brain sections from TgCRND8 mice that had been triple-labeled with Thioflavin-S, thionin and DAB/p-p38(MAPK) were examined in more detail. The p-p38(MAPK) cells surrounding the outside of 'dense-core' plaques formed a radial pattern of distribution (Figure 14). As expected, the size of Thioflavin-S and thionin staining positive cores tended to increase in parallel, while 'dense-core' plaques tended to be the predominant form of plaque associated with p-p38(MAPK)-IR cells (Figure 14A-D). These changes also correlated with the mean number of p-p38(MAPK)-IR cells and the absolute core size. Interestingly, the mean number of p-p38(MAPK)-IR cells and the proportional core size was negatively correlated, e.g. the number of p-p38(MAPK)-IR cells decreased when the Thioflavin-S- and thionin-positive core occupied a higher percentage area of the absolute plaque area.

However, an additional and very exciting observation was made. Indeed, in Figure 12C (above), the mean number of p-p38(MAPK)-IR cells decreased as a function of plaque area (an effect that was iterated in the correlation data presented in Figure 13).

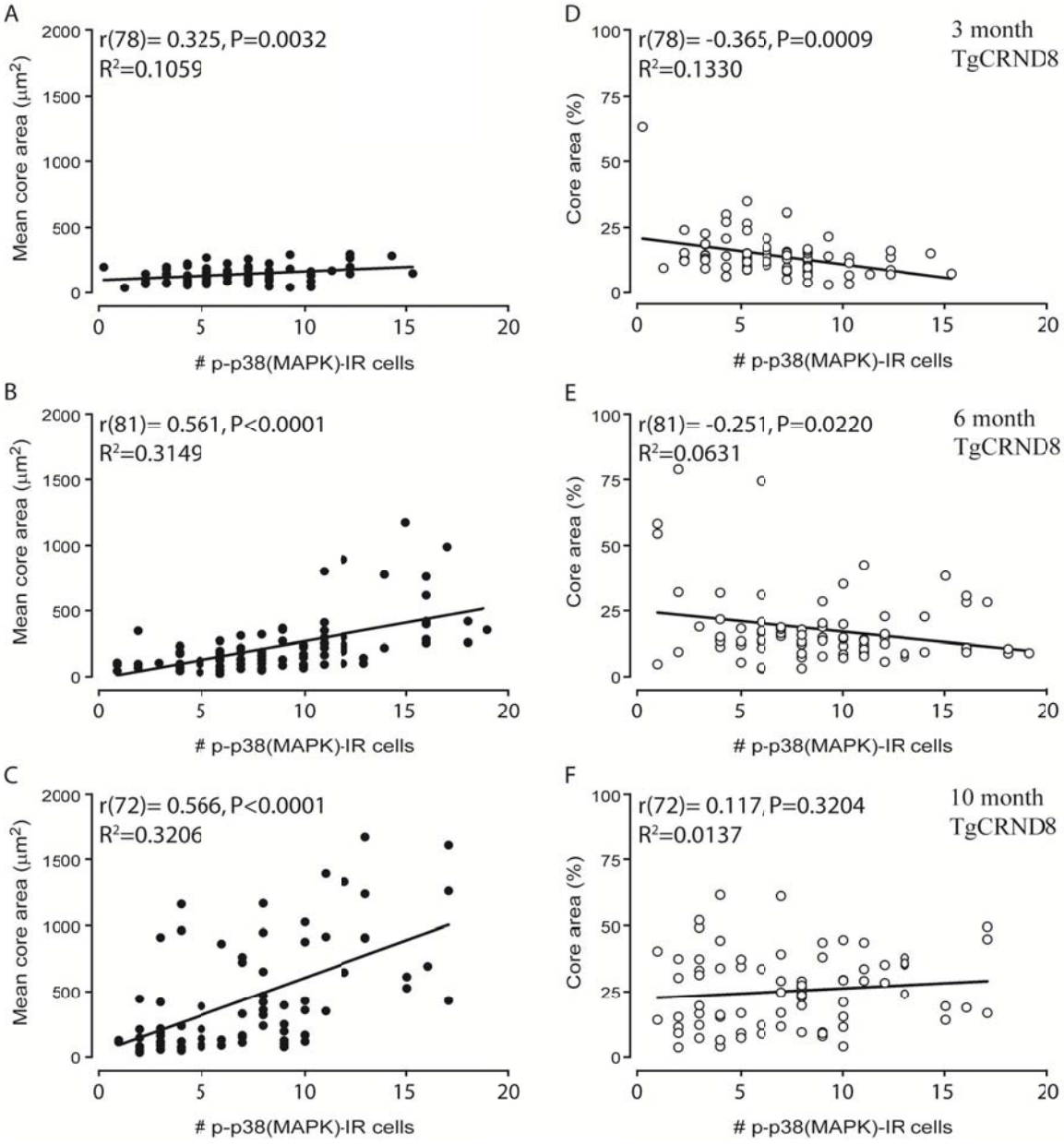
A
r(78)= 0.325, P=0.0032
R²=0.1059
Mean core area (µm²)
# p-p38(MAPK)-IR cells
B
r(81)= 0.561, P<0.0001
R²=0.3149
Mean core area (µm²)
# p-p38(MAPK)-IR cells
C
r(72)= 0.566, P<0.0001
R²=0.3206
Mean core area (µm²)
# p-p38(MAPK)-IR cells
D
r(78)= -0.365, P=0.0009
R²=0.1330
3 month
TgCRND8
Core area (%)
# p-p38(MAPK)-IR cells
E
r(81)= -0.251, P=0.0220
R²=0.0631
6 month
TgCRND8
Core area (%)
# p-p38(MAPK)-IR cells
F
r(72)= 0.117, P=0.3204
R²=0.0137
10 month
TgCRND8
Core area (%)
# p-p38(MAPK)-IR cells

(Previous page)

---

**Figure 13. The correlation between the mean number of p-p38(MAPK)-IR cells with absolute core size and proportional core size.** 3-, 6- and 10-month TgCND8 mice were used. The data depicted in panels A/D, B/E, C/F were obtained from 3-, 6-, 10-month-old TgCRND8 mice, respectively. (A-C) The mean number of p-p38(MAPK)-IR cells is positively correlated with absolute core size and the correlation enhances with age. (D-F) The number of p-p38(MAPK)-IR cells is inversely related to the size of the core as a function of the size of the overall plaque and the correlation is lost with age. $n$ = 3-4 animals. Statistical summaries are included in the individual panels with 'r': correlation coefficient; P: is the probability value (e.g. significant if $\leq 0.05$); $R^2$: is the square of the 'r' value and helps with the interpretation of the data. For example, in panel C, an $R^2$ value of 0.3206 means that 32% of the variance in the number of p-p38(MAPK)-IR cells can be explained by variation in in the size of the mean core area.

In keeping with this, Figure 14C/C′, 14D/D′ clearly suggest that p-p38(MAPK)-IR cells may restrict the core maturation and development. Indeed, these images reveal that if a core within a plaque is surrounded with the radially distributed p-p38(MAPK)-IR cells, the extension of the core is restricted more or less by the cells (Figure 14A/A′, B/B′). However, if p-p38(MAPK)-IR cells were no longer present around a plaque, the core within this plaque tended to expand outward along the aspect of the plaque that was now devoid of p-p38(MAPK)-IR cells. Moreover, in superficial parts of the sensorimotor cortex where there are very few, if any, p-p38(MAPK-IR cells (Figure 15A and 15A′), what were initially identified as thionin-positive deposits (reminiscent of amyloid deposits), were subsequently identified, using Thioflavin-S staining, to be uncontrolled growing and amorphic 'dense-core' plaques. These kinds of 'dense-core' plaques were devoid of p-p38(MAPK)-IR cells, which strongly suggested that the p-p38(MAPK)-IR cells were not necessarily causing the recruitment of Aβ into the plaques. Given that the amyloid core expanded along the aspect that was devoid of p-p38(MAPK)-IR cells, and that fibrillar Aβ aggregated to plaques in the absence of plaque-associated p-p38(MAPK)-IR cells, these observations strongly supported the potential that p-p38(MAPK)-IR cells could be playing a greater role in restricting the maturation of Thioflavin-S-positive core than in promoting the growth of 'dense-core' plaques.

### 3.6 Identification of the phenotype of p-p38(MAPK)-IR cells via using double immunofluorescence

The literature shows that amyloid plaques are associated with the activation and proliferation of microglia and astrocytes [127, 128]. As well, p-p38(MAPK)-IR has been observed in the activated microglia, astrocytes and neurons that surround senile plaques in the hippocampus of TgCRND8 mice [118]. Therefore, it was important to identify the phenotype of p-p38(MAPK)-IR cells that localized to amyloid plaques in the sensorimotor cortex of TgCRND8 mice. Not only would this benefit the current project, but it would also assist in our understanding of the role of p-p38(MAPK) in AD-related pathology. To determine the phenotype of p-p38(MAPK)-IR cells, double immunofluorescence with the anti-p-p38(MAPK) antibody and several cell markers were

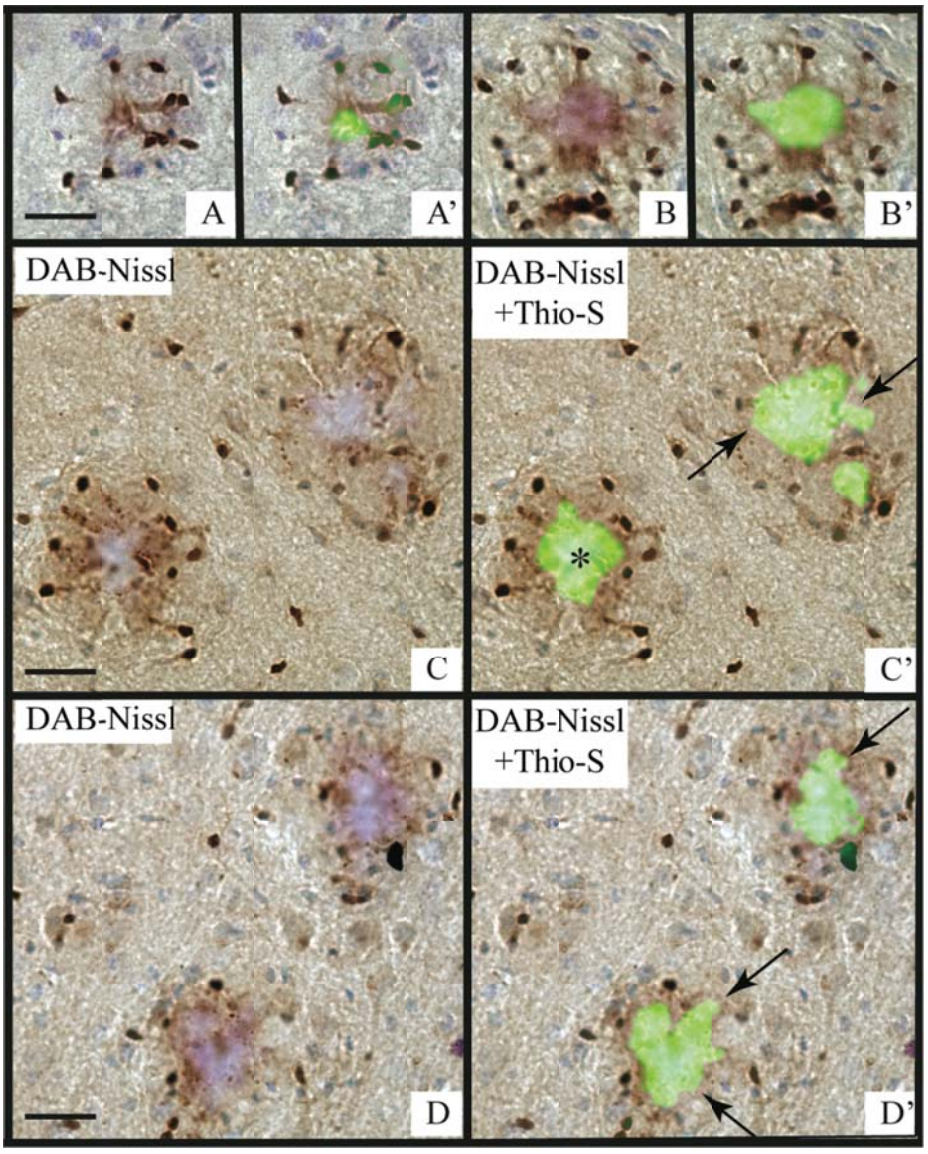
A
A'
B
B'
DAB-Nissl
DAB-Nissl
+Thio-S
*
C
C'
DAB-Nissl
DAB-Nissl
+Thio-S
D
D'

(Previous page)

---

**Figure 14. The loss of p-p38(MAPK)-IR cells around a 'dense-core' plaque coincides with the expansion of Thioflavin-S-positive core.** Sections from 3- and 10-month TgCRND8 mice were triple labeled by thioflavin-S staining, thionin/Nissl staining and DAB-immunohistochemistry with the p-p38(MAPK) antibody. Panels A/A′ and B/B′ represent fields within cortical sections from 3-month mice whereas panels C/C′ and D/D′ represent fields within cortical sections from 10-month mice. 'Dense-core' plaques are visualized by both Thioflavin-S (green) and thionin (purple) staining. DAB-immunohistochemistry (brown) clearly shows the distribution of p-p38(MAPK)-IR cells. The loss of p-p38(MAPK)-IR cells in the vicinity of plaques allows the Thioflavin-S-positive cores to grow out uncontrollably along the aspect devoid of p-p38(MAPK)-IR cells (arrows). Asterisk indicates a 'restricted' core within a 'dense-core' plaque surrounded by radially distributed p-p38(MAPK) cells. Scale bars, 20 μm.

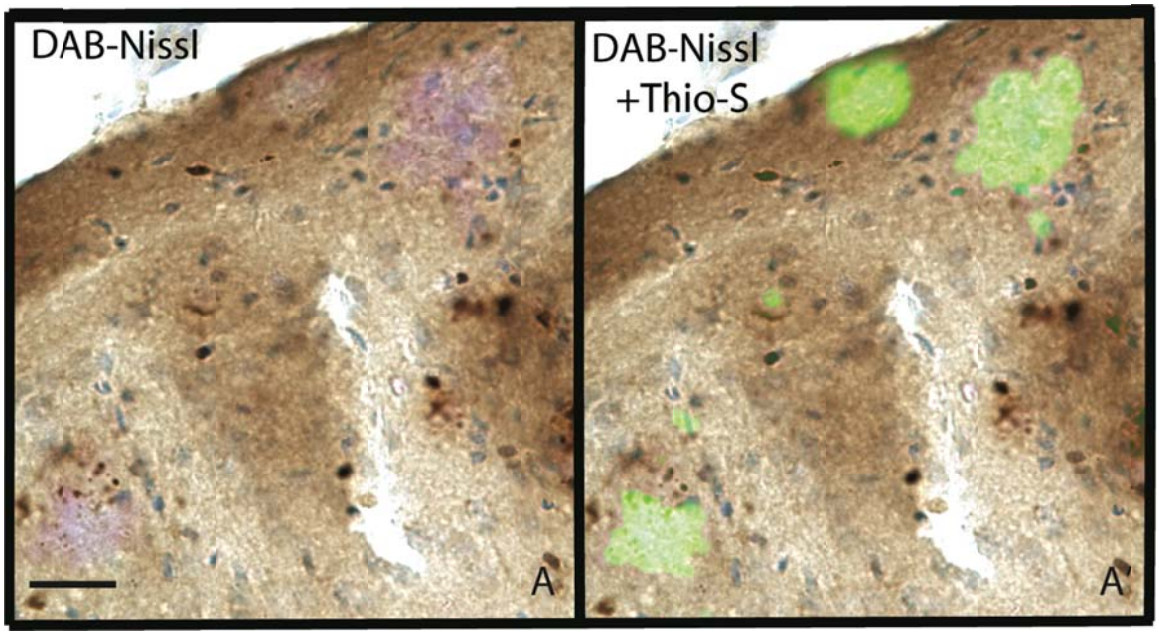


**Figure 15. Uncontrolled growth of 'dense-core' plaques was detected by thionin and Thioflavin-S staining.** Purple patches were observed in the superficial layers of the cortex by thionin/Nissl staining and then confirmed to be 'dense-core' plaques by Thioflavin-S staining. The sections were also processed for p-p38(MAPK) DAB-immunohistochemistry. These amorphic 'dense-core' plaques are clearly devoid of p-p38(MAPK)-IR cells. Scale bar, 25 μm.

visualized under confocal microscopy. The cell marker antibodies included NeuN (neurons), GFAP (astrocytes), ED-1 and Mac-1 (both of ED-1 and Mac-1 detect microglia, but the two antibodies selectively recognize different types of microglia or microglia in different stages). p-p38(MAPK)-IR was rarely detected in GFAP-positive astrocytes and occasionally observed in NeuN-positive neurons (Figure 16). Although there was evidence of some p-p38(MAPK) expressing in the ED-1-positive microglia, the majority of p-p38(MAPK) were detected in the Mac-1-positive microglia. In addition, the Mac-1-positive, p-p38(MAPK)-IR cells were present in parenchyma of both wildtype and TgCRND8 mice, and were clearly detetcted around the 6E10-positive plaques (Figure 16). The p-p38(MAPK)-IR signal was observed in both cytoplasm and nucleus in cells, whereas (as expected) Mac-1 predominately labeled the plasma membrane. These data confirmed that p38(MAPK) can be constitutively phosphorylated in parenchymal microglia in both wildtype or TgCRND8 mouse cortex, and a higher intensity of p-p38(MAPK)-IR, Mac-1-positive microglia were observed in the vicinity of amyloid plaques in the sensorimotor cortex of TgCRND8 mice (Figure 16, 17).

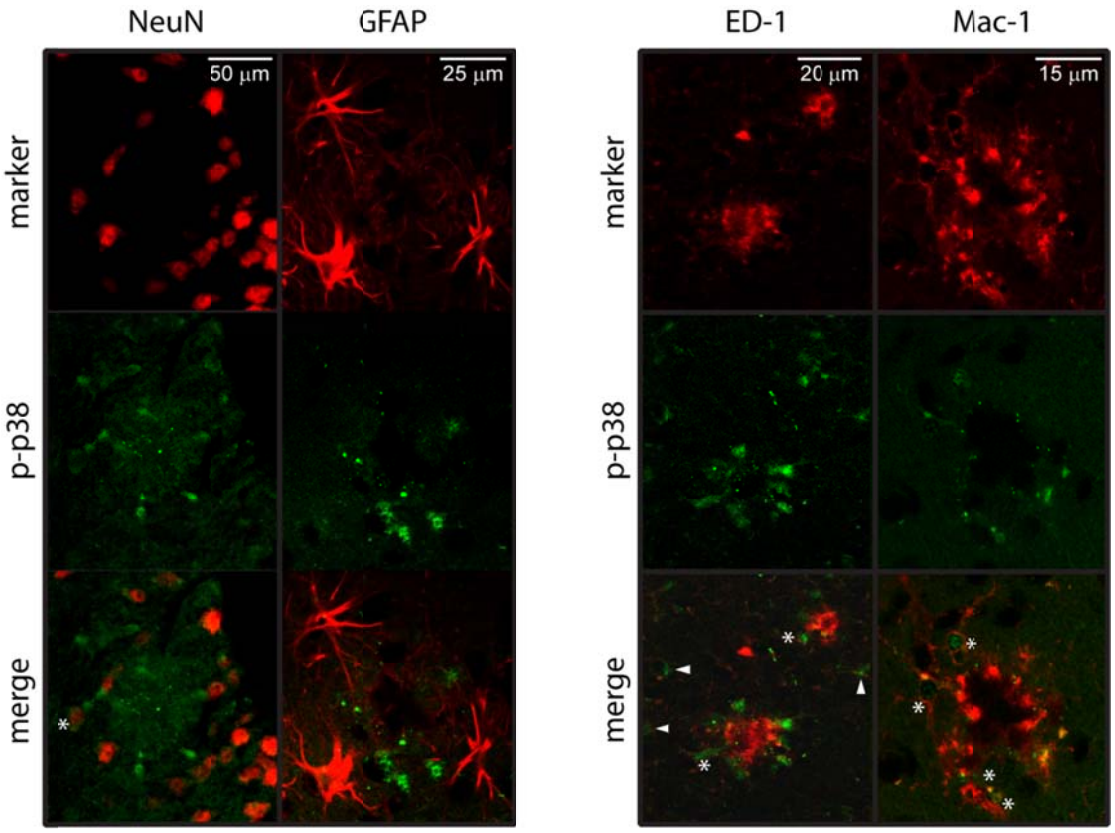


**Figure 16. Plaque-associated p-p38(MAPK)-IR cells are predominately microglia that stain positive for Mac-1 marker.** Sections from 10-month-old TgCRND8 mice were probed for p-p38(MAPK) (green, in all four columns) and NeuN (red, first column), GFAP (red, second column), ED-1 (red, third column) or Mac-1 (red, fourth column) by immunofluorescence. p-p38(MAPK)-IR cells are detected in NeuN-positive neurons occasionally, rarely in GFAP-positive astrocytes, sometimes in ED-1-positive microglia and more frequently in Mac-1-positive microglia. Asterisks indicates that signals of p-p38(MAPK). The various cell markers are observed in same cells. In contrast, arrowheads indicate those cells positive for the respective marker (e.g. ED-1), but devoid of any signal for p-p38(MAPK).

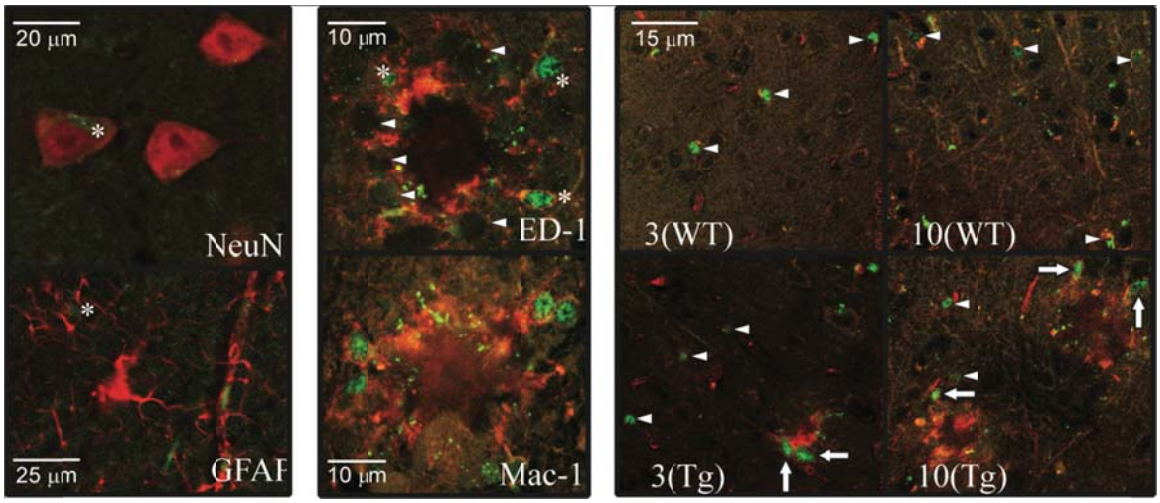


**Figure 17. Plaque-associated p-p38(MAPK)-IR cells are predominately Mac-1-positive microglia and p-p38(MAPK)-IR/Mac-1-positive microglia are detected in both cortical parenchyma and in the vicinity of plaques cortex.** Although the occasional GFAP-positive or NeuN-positive cell also is positive for p-p38(MAPK) (left panel), higher magnification images clearly identifies p-p38(MAPK)-IR cells as predominantly Mac-1-positive, and not ED-1-positive, microglia (middle panel). (right panel) 3- and 10-month wildtype and TgCRND8 mice were double labeled with anti-p-p38(MAPK) (green) and Mac-1 (red) antibodies. p-p38(MAPK) immunoreactivity was observed in parenchymal cells as well as the Mac-1 signal (arrowheads), but a higher number of cells double-labeled with both p-p38(MAPK) (with a greater intensity of signal) and Mac-1 were detected around amyloid plaques (arrows).

### 3.7 The association between p-p38(MAPK)-IR cells and amyloid plaques in the sensorimotor cortex

Based on the previous data, although p-p38(MAPK) can be phosphorylated in the parenchyma of cortex, a higher intensity of p-p38(MAPK)-IR cells were observed in the vicinity of amyloid plaques. The quantification and analyses of the parameters of p-p38(MAPK)-IR cells and amyloid plaques revealed that the number of p-p38(MAPK)-IR cells changed with plaque size and core size. Therefore, as a logical conclusion to this project, sections from 6- and 10-month TgCRND8 mice were chosen for double-labeling with anti-p-p38(MAPK) and 6E10 (anti-APP) antibodies. The association of p-p38(MAPK)-IR cells and 6E10-positive amyloid plaques was then examined using immunofluorescence. Under the 60X objective, the localization of p-p38(MAPK)-IR cells to 6E10-positive amyloid plaques was observed. Most of the p-p38(MAPK)-IR cells surrounded the periphery of the plaque, yet some of the processes of these p-p38(MAPK)-IR cells extended through the outer part of the 6E10-positive plaque and ended within the Thioflavin-S-positive core area (Figure 18). In addition, the areas immediately peripheral to the plaque that were occupied by p-p38(MAPK)-IR cells were devoid of 6E10 signal. These data provided evidence to suggest that these Mac-1/p-p38(MAPK)-IR cells are not simply 'resting' when they are in the vicinity of an amyloid plaques, but that they must, in fact, be influencing certain aspects of amyloid load (deposition/removal) (Figure 18). This notion was further supported by images taken at higher magnification (i.e. 100X objective) (Figure 19). The p-p38(MAPK)-IR microglia were scanned from bottom to top (along the Z-axis) at 1 μm intervals and a series of images was obtained representing serial sections of the p-p38(MAPK)-IR microglia. In these images, the 6E10 signal was detected in the p-p38(MAPK)-IR microglia, suggesting that the Aβ from the amyloid plaques was being taken into the p-p38(MAPK)-IR microglia (Figure 19). Note that these experiments do not indicate at this point whether this Aβ is simply sequestered or if it is subsequently degraded.

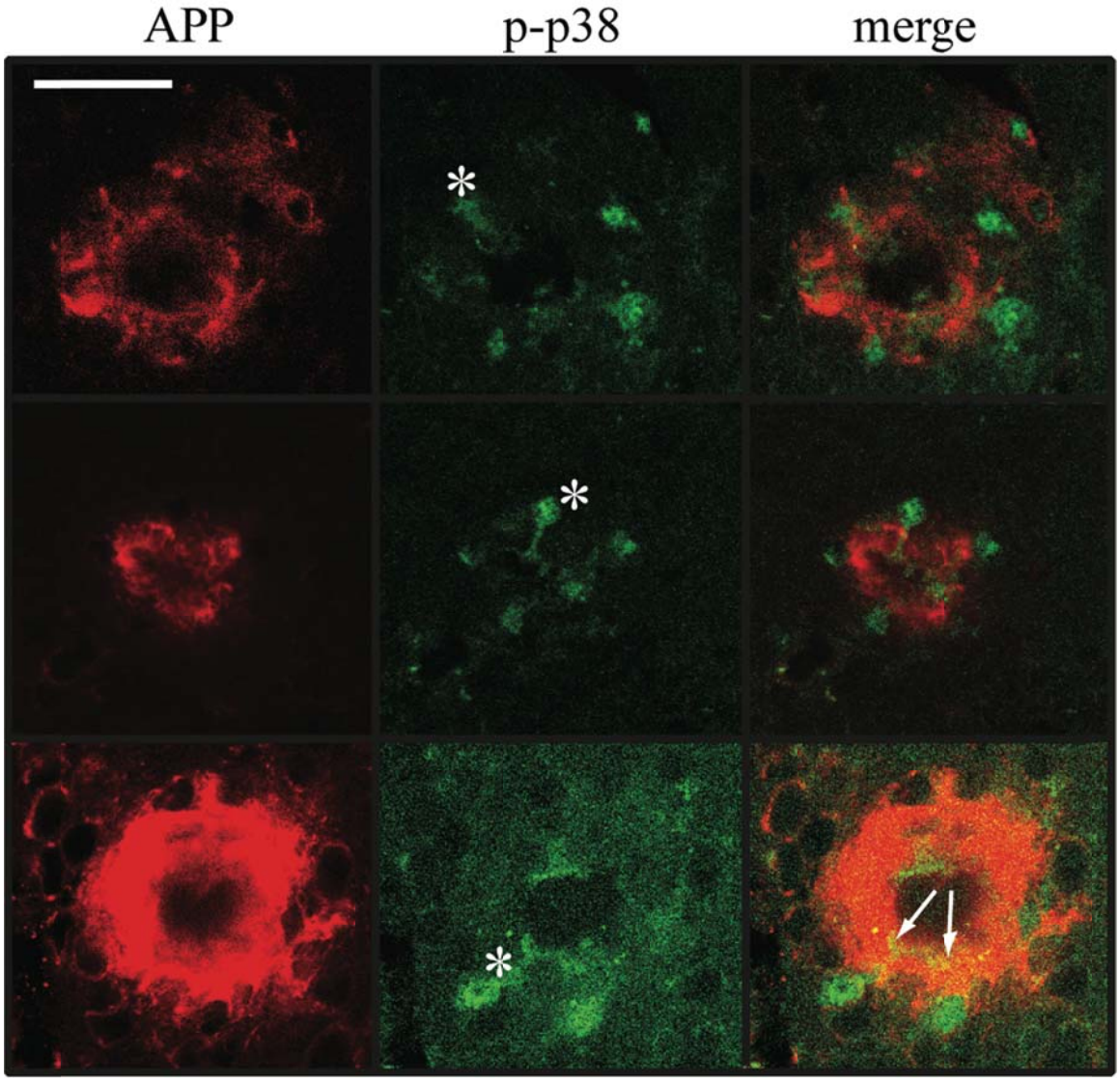


**Figure 18. The p-p38(MAPK)-IR cells extend into the core area.** p-p38(MAPK)-IR cells and amyloid plaques were respectively detected by anti-p-p38(MAPK) (green) and 6E10 (anti-APP: red) antibodies using immunofluorescence. The radial distribution of p-p38(MAPK)-IR cells is observed around 'dense-core' plaques and the areas with p-p38(MAPK)-IR cells are much less 6E10 signal, suggesting local removal of Aβ. Moreover, p-p38(MAPK)-IR cells are not simply surrounding the 'dense-core' plaques, but extend into the core area. Scale bar, 10 μm.

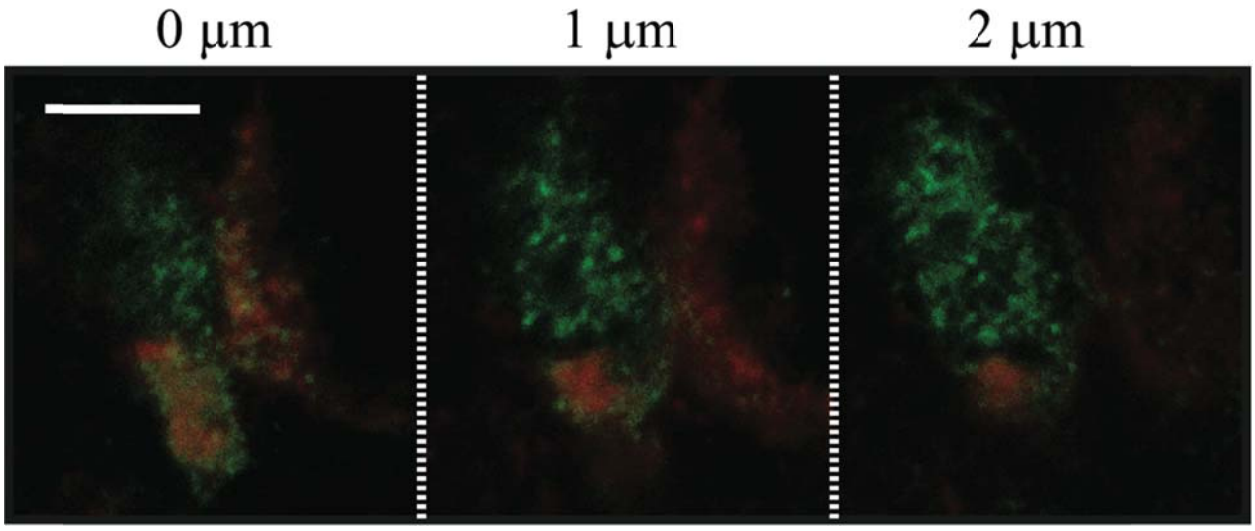


**Figure 19. Serial images reveal the presence of Aβ in a p-p38(MAPK)-IR cell.** Section was probed for p-p38(MAPK) (green) and Aβ (using the 6E10 antibody: red). Three confocal images collected along the z-axis at 1 μM intervals revealed that the Aβ from the adjacent plaque (the crescent-shaped structure alongside the p-p38(MAPK)-IR cell) is detected in the p-p38(MAPK)-IR cell. Scale bar, 3 μm.

## 4. DISCUSSION

In this project, I chose to examine the sensorimotor cortex of wildtype and TgCRND8 mice because disruptions in the function of this structure have recently been associated with cognitive impairment during the progression of AD [135, 136]. For example, Frisoni et al (2009) reported a progressive grey matter loss of 7-9% and 10-11% in the sensorimotor cortex in mild and moderate AD, respectively. The amyloid plaques formed during AD are thought to provoke inflammatory responses which are detrimental to the surrounding brain tissue. The recruitment of microglia and astrocytes is a key component of the inflammatory response. Since increased numbers of microglia and astrocytes are observed surrounding amyloid plaques in AD, the increased p38(MAPK) signaling detected in these microglia and astrocytes is believed to contribute to both the development of the plaques and the disruption of the surrounding parenchymal tissue [115, 137, 138]. This notion of a detrimental role for p38(MAPK) is further supported by the finding that p38(MAPK) activity is associated with inflammatory signals and apoptosis [114, 128, 139, 140]. Reports have suggested that p-p38(MAPK) is primarily involved in proinflammatory responses, although it can also regulate the biosynthesis and expression of the inflammatory cytokines [69, 141]. On the other hand, others believe that the recruitment of microglia to the vicinity of amyloid plaques could be beneficial in AD by reducing the Aβ burden and retarding the plaque development [118, 142, 143]. While the initial examinations confirmed the presence of p-p38(MAPK)-IR cells in the sensorimotor cortex of wildtype and TgCRND8 mice and subsequently identified these cells as [predominantly] microglia, it was still unclear whether these p-p38(MAPK)-IR microglia were exerting harmful or beneficial effects with regard to the amyloid plaque. Therefore, quantification of the data over a span of ages was used to help understand the changes, if any, in distribution, localization and concentration of these cells with respect to the amyloid plaques.

### 4.1 The presence of p-p38(MAPK)-IR microglia throughout the parenchyma of cortex in both wildtype and TgCRND8 mice suggests a non-pathological role for these cells.

p-p38(MAPK)-IR microglia were detected across the parenchyma of the sensorimotor cortex in 3-, 6- and 10-month wildtype and TgCRND8 mice using DAB-immunohistochemistry (Figure 9). Parenchymal p-p38(MAPK)-IR microglia had already been demonstrated in cortex and hippocampus of these mice. In those published studies, there were more p-p38(MAPK)-IR cells as well as a greater intensity of the p-p38(MAPK) signal in TgCRND8 than in wildtype mice [115, 118]. In the current project, an apparently evenly distributed pattern of p-p38(MAPK)-IR microglia in cortical parenchyma was observed and the presence of parenchymal p-p38(MAPK)-IR cells was confirmed stereologically in both wildtype and TgCRND8 mice (i.e. independent of genotype) (Figure 11). Moreover, stereological sampling revealed that the number and density of these parenchymal p-p38(MAPK)-IR microglia also remained unaffected as a function of age in wildtype mice (Figure 11A). This evidence suggests that p38(MAPK) can be constitutively phosphorylated in microglia across the cortical mantle and that the density of these activated p38(MAPK)-IR microglia is not affected by either genotype or age. It is interesting that the density of parenchymal p-p38(MAPK)-IR microglia was unaffected by either the presence or density of amyloid plaques or by the localization of a significant number of p-p38(MAPK)-IR microglia to the vicinity of amyloid plaques. Even in 10-month-old TgCRND8 mice, the parenchymal p-p38(MAPK)-IR microglia maintained the same pattern of distribution and same level of expression, although the number of amyloid plaques and plaque-associated p-p38(MAPK)-IR microglia was greatly increased. Therefore, in comparison to the plaque-associated p-p38(MAPK)-IR cells, the parenchymal pool of p-p38(MAPK)-IR microglia can be considered as 'resting', with little or no apparent direct influence on the development of amyloid plaques [144, 145]. It is assumed that the plaque-associated p-p38(MAPK)-IR microglia originate from this parenchymal pool, but this was not confirmed during the course of the present series of experiments. In fact, the literature does indicate that bone marrow-derived microglia have different inherent properties than the 'resident' microglia in the brain and that these bone marrow-derived microglia can participate in the response to

amyloid deposition [146]. When the bone marrow-derived microglia are diminished in an animal model of AD-related pathology, the number of plaque-associated microglia is decreased and the development of dense-core plaques is accelerated [142, 147]. The current observations support parenchymal p-p38(MAPK)-IR microglia as being 'resting' and of playing a non-pathological role, perhaps contributing simply to the homeostatic maintenance of the brain. It is unclear at this time whether parenchymal p-p38(MAPK)-IR microglia from other sources are being recruited in response to the development of the amyloid plaques in the TgCRND8 mouse model of AD-related pathology.

### 4.2 The density of plaque-associated p-p38(MAPK)-IR microglia is inversely related to the size of Thioflavin-S-positive cores.

The plaque-associated p-p38(MAPK)-IR microglia were detected in the vicinity of both dense-core and diffuse plaques (Figure 10), but stereological sampling indicated that the number of p-p38(MAPK)-IR microglia more closely related with the dense-core plaques. The density of plaque-associated p-p38(MAPK)-IR microglia increased in the cortex with genotype and age in parallel with the increase in the number and size of dense-core plaques in the same area (Figure 11A, 11B and 12A). The presence of dense-core plaques suggests that the Aβ in this area is aggregating and undergoing a transition to the fibrillar conformation. The presence of these plaques is often associated with inflammatory pathology that could activate the p38(MAPK) signaling in microglia and recruit these cells to the general vicinity of the plaques. As a result, it could be assumed that an increase in the number of amyloid plaques could account for the higher density of p-p38(MAPK)-IR microglia localized to the vicinity of these plaques in the sensorimotor cortex. However, when I focused on the individual dense-core plaques, the number of p-p38(MAPK)-IR microglia per dense-core plaque showed a significant increase in 6-month-old TgCRND8 mice, whereas the number stabilized or even decreased slightly in the 10-month-old TgCRND8 mouse cortex (Figure 12B). Although the number of both plaque-associated p-p38(MAPK)-IR microglia and dense-core plaques increased with age in the cortex, differences of the increasing rate were revealed in the different periods (Figure 11A and 11 B). The increase in density of the dense-core plaques between the 6-

month and 10-month TgCRND8 cortices paralleled a decline in plaque-associated p-p38(MAPK)-IR microglia and was more significant than the increase in density dense-core plaques from the 3-month to the 6-month cortices. Therefore, the p-p38(MAPK)-IR microglia were apparently involved in something different in TgCRND8 mice between 3- and 6-months of age and 6- and 10-months of age. Stereology subsequently revealed that the number of p-p38(MAPK)-IR microglia localized to an individual dense-core plaque dense-core plaque tended to correlate with the size of the individual plaque, but that the actual size of the dense core of a plaque tended to increase in those plaques with fewer associated p-p38(MAPK)-IR microglia (Figure 13). So as to better understand what could be transpiring in these mice, the size of individual dense cores was expressed as 'absolute' (actual size) and 'proportional' (in relation to the size of the surrounding plaque), and the correlation of the density of p-p38(MAPK)-IR microglia with the two kinds of core size was evaluated. The larger dense-core plaques associated with a lower density of plaque-associated p-p38(MAPK)-IR microglia in the older transgenic mice, which indicated the development (number and size) of dense-core plaques was inversely related with the density of p-p38(MAPK)-IR microglia. This finding is consistent with a previous report that demonstrated that the induction of plaque-associated cells restricts the development of dense-core plaques [148]. In the current study, the Thioflavin-S-positive core expended along the aspects that were devoid of p-p38(MAPK)-IR microglia and amorphic dense-core plaques without radially distributed p-p38(MAPK)-IR microglia were detected in the superficial layers of cortex (Figure 14C, D and E). Thus, p-p38(MAPK)-IR microglia appear to play a role in restricting the maturation and growth of the cores, rather than on the aggregation and development of the amyloid deposit itself. While these observation were quite evident in 10-month TgCRND8 mice, it should be noted that there were still a number of large plaques (with smaller cores) that were ringed by a high number of p-p38(MAPK)-IR microglia. Therefore, not all plaques responded in a similar manner [perhaps due to the cortical layer within which they resided and the local microenvironment or perhaps due to differences in the type and/or function of the local cell population] and not all p-p38(MAPK)-IR cells were 'removed' (re-localized away from the plaque or simply inactivated) simultaneously. The reason for this remains unclear.

### 4.3 p-p38(MAPK)-IR microglia may facilitate the phagocytosis and clearance of Aβ deposits

The radial distribution of plaque-associated p-p38(MAPK)-IR microglia around dense-core plaques included cells whose processes extended into the Thioflavin-S-positive core area. Besides, when we detected some plaque-associated p-p38(MAPK)-IR microglia located at the penumbra (non-fibrillar area) of dense-core plaques, the immediate areas adjacent to the p-p38(MAPK)-IR microglia were often devoid of 6E10/Aβ immunoreactivity (Figure 18). This observation suggested that p-p38(MAPK)-IR microglia could be helping to clear Aβ. A series of confocal microscopic images revealed that the 6E10 (e.g. anti-APP/Aβ) signal could be detected within the margins of the p-p38(MAPK-IR microglia (Figure 19), thus strongly supporting the uptake of Aβ into p-p38(MAPK)-IR microglia, presumably via a phagocytotic process. This corroborated a previous report of p-p38(MAPK)-IR microglia clearing Aβ deposits and potentially even denaturing and removing the aggregated/fibrillar form of Aβ [149].

### 4.4 The origins of parenchymal and plaque-associated p-p38(MAPK)-IR microglia

When the number of plaque-associated p-p38(MAPK)-IR microglia increased with age and genotype, there was not a corresponding decrease in the parenchymal pool of p-p38(MAPK)-IR microglia. Three possibilities could explain this observation. First, the parenchymal p-p38(MAPK)-IR microglia were recruited to the vicinity of the amyloid plaques and then a new population of parenchymal p-p38(MAPK)-IR microglia was activated. Second, the increased number of plaque-associated p-p38(MAPK)-IR cells were derived from other sources, such as blood vessels and bone marrow. Lastly, the new population of plaque-associated p-p38(MAPK)-IR microglia were derived from local mitosis. Given that the resting form of parenchymal p-p38(MAPK)-IR microglia did not changes with age or genotype, and that the overall distribution of these cells was not disturbed by the presence of the amyloid plaque or plaque-associated p-p38(MAPK)-IR microglia, this would suggest that the increased number of plaque-associated p-p38(MAPK)-IR microglia were probably not originating from the parenchymal pool of p-

p38(MAPK)-IR microglia. However, previous studies have revealed that 5-bromo-2′-deoxyuridine (BrdU)-positive microglia could be detected in the vicinity of dense-core plaque and as such the local mitosis of p-p38(MAPK)-IR microglia could contribute to the increased number of plaque-associated p-p38(MAPK)-IR microglia [150]. Finally, several p-p38(MAPK)-IR microglia were observed within the blood vessels in the sensorimotor cortex (Figure 10). This observation corroborates several other reports and indicates the peripheral vasculature can be an origin of the population of plaque-associated p-p38(MAPK)-IR microglia [137, 142].

## 5. FUTURE WORK

Our laboratory recently observed that p-p38(MAPK) could affect the function of a mitochondrial enzyme, monoamine oxidase-A (MAO-A) [116]. Interestingly, MAO-A generates hydrogen peroxide as a reaction by-product and because of its potential for inducing oxidative stress, MAO-A has been forwarded as a candidate for increasing the vulnerability of cells during the progression of AD [151-153]. With this in mind, I used immunofluorescence to examine the distribution of MAO-A using two different antibodies (H-70 and T-19) in the sensorimotor cortex of wildtype and TgRND8 mice, and co-labeled with p-p38(MAPK), Mac-1 or NeuN antibodies in the same sections. I was not able to conclusively identify Mac-1-positive cells that were positive for both p-p38(MAPK) and MAO-A. As such, my initial observations do not support the co-expression of these two proteins in plaque-associated, Mac-1-positive cells (Figure 20). However, MAO-A (Figure 20) could be detected in neurons (NeuN-positive cells). Given that I had previously detected p-p38(MAPK) in NeuN-positive cells (Figure 17), this supports the possibility that a population of p-p38(MAPK)-IR neurons could be influenced by the local activity of MAO-A and could help to link these two proteins, i.e. p-p38(MAPK) and MAO-A, in the context of AD-related pathology. As such, I suggest that the roles of p-p38(MAPK) and MAO-A, and the exciting possibility that these two proteins could be interacting in these neurons, should be examined further in AD-related mouse models, including the TgCRND8 mouse.

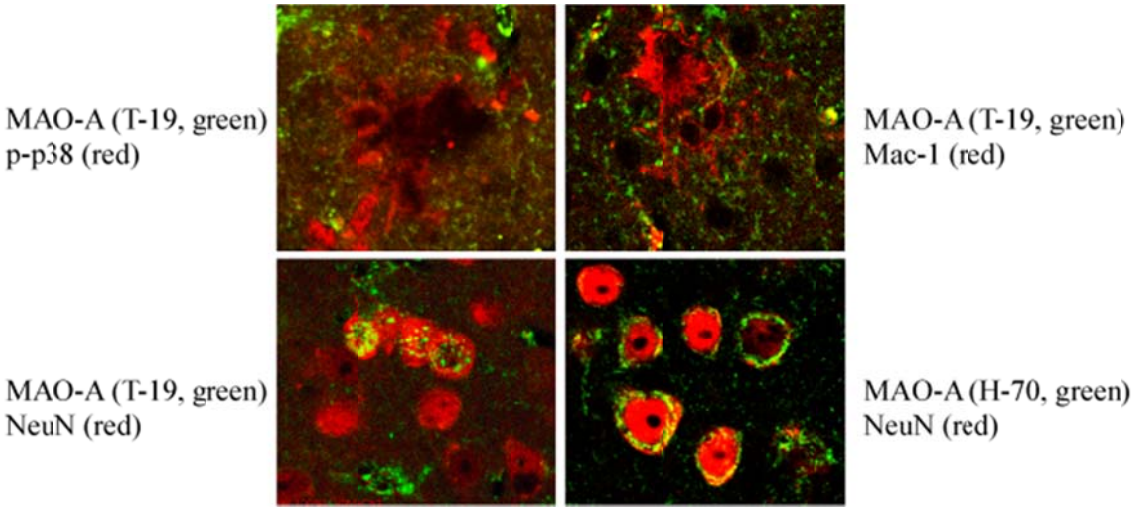


**Figure 20. MAO-A is detected primarily in NeuN-positive cells.** ***(top)*** There is very little detection of MAO-A within either p-p38(MAPK)- or Mac-1-positive cells. ***(bottom)*** Both of the MAO-A antibodies gave a strong signal in NeuN-positive cells (neurons) in mouse cortex.

## REFERENCES


1. M Goedert, MG Spillantini: **A century of Alzheimer's disease**. *Science* 2006, **314**:777-81.
2. NC Berchtold, CW Cotman: **Evolution in the conceptualization of dementia and Alzheimer's disease: Greco-Roman period to the 1960s**. *Neurobiology of aging* 1998, **19**:173-89.
3. EM Ebly, IM Parhad, DB Hogan, TS Fung: **Prevalence and Types of Dementia in the Very Old - Results from the Canadian-Study-of-Health-and-Aging**. *Neurology* 1994, **44**:1593-1600.
4. R Brookmeyer, E Johnson, K Ziegler-Graham, HM Arrighi: **Forecasting the global burden of Alzheimer's disease**. *Alzheimer's & dementia : the journal of the Alzheimer's Association* 2007, **3**:186-91.
5. L Bertram, RE Tanzi: **Thirty years of Alzheimer's disease genetics: the implications of systematic meta-analyses**. *Nature reviews. Neuroscience* 2008, **9**:768-78.
6. BA Yankner: **Decoding darkness: The search for the genetic causes of Alzheimer's disease**. *Nature* 2000, **408**:31-32.
7. SC Waring, RN Rosenberg: **Genome-wide association studies in Alzheimer disease**. *Archives of Neurology* 2008, **65**:329-34.
8. H Forstl, A Kurz: **Clinical features of Alzheimer's disease**. *European archives of psychiatry and clinical neuroscience* 1999, **249**:288-90.
9. E Arnaiz, O Almkvist: **Neuropsychological features of mild cognitive impairment and preclinical Alzheimer's disease**. *Acta neurologica Scandinavica. Supplementum* 2003, **179**:34-41.
10. G Waldemar, B Dubois, M Emre, J Georges, IG McKeith, M Rossor, P Scheltens, P Tariska, B Winblad: **Recommendations for the diagnosis and management of Alzheimer's disease and other disorders associated with dementia: EFNS guideline**. *European journal of neurology : the official journal of the European Federation of Neurological Societies* 2007, **14**:e1-26.
11. L Nygard: **Instrumental activities of daily living: a stepping-stone towards Alzheimer's disease diagnosis in subjects with mild cognitive impairment?** *Acta neurologica Scandinavica. Supplementum* 2003, **179**:42-6.
12. EM Frank: **Effect of Alzheimer's disease on communication function**. *Journal of the South Carolina Medical Association* 1994, **90**:417-23.
13. DP Gold, MF Reis, D Markiewicz, D Andres: **When Home Caregiving Ends - a Longitudinal-Study of Outcomes for Caregivers of Relatives with Dementia**. *Journal of the American Geriatrics Society* 1995, **43**:10-16.
14. DJ Selkoe: **Alzheimer's disease: genes, proteins, and therapy**. *Physiological reviews* 2001, **81**:741-66.
15. M Goedert, MG Spillantini, RA Crowther: **Tau proteins and neurofibrillary degeneration**. *Brain pathology* 1991, **1**:279-86.
16. W Chun, GV Johnson: **The role of tau phosphorylation and cleavage in neuronal cell death**. *Frontiers in bioscience : a journal and virtual library* 2007, **12**:733-56.
17. J Hardy, D Allsop: **Amyloid Deposition as the Central Event in the Etiology of Alzheimers-Disease**. *Trends in Pharmacological Sciences* 1991, **12**:383-388.
18. DJ Selkoe: **The molecular pathology of Alzheimer's disease**. *Neuron* 1991, **6**:487-98.
19. S Yoshikai, H Sasaki, K Doh-ura, H Furuya, Y Sakaki: **Genomic organization of the human-amyloid beta-protein precursor gene**. *Gene* 1991, **102**:291-2.

20. C Priller, T Bauer, G Mitteregger, B Krebs, HA Kretzschmar, J Herms: **Synapse formation and function is modulated by the amyloid precursor protein**. *Journal of Neuroscience* 2006, **26**:7212-7221.
21. T Hartmann, SC Bieger, B Bruhl, PJ Tienari, N Ida, D Allsop, GW Roberts, CL Masters, CG Dotti, K Unsicker, et al: **Distinct sites of intracellular production for Alzheimer's disease A beta40/42 amyloid peptides**. *Nature medicine* 1997, **3**:1016-20.
22. JS Verbeek, WL Hazenbos, PJ Capel, JG van de Winkel: **The role of FcR in immunity: lessons from gene targeting in mice**. *Research in immunology* 1997, **148**:466-74.
23. J Nunan, DH Small: **Regulation of APP cleavage by alpha-, beta- and gamma-secretases**. *FEBS letters* 2000, **483**:6-10.
24. MS Wolfe: **The gamma-secretase complex: membrane-embedded proteolytic ensemble**. *Biochemistry* 2006, **45**:7931-9.
25. YI Yin, B Bassit, L Zhu, X Yang, C Wang, YM Li: **{gamma}-Secretase Substrate Concentration Modulates the Abeta42/Abeta40 Ratio: IMPLICATIONS FOR ALZHEIMER DISEASE**. *The Journal of biological chemistry* 2007, **282**:23639-44.
26. DW Dickson: **The pathogenesis of senile plaques**. *Journal of neuropathology and experimental neurology* 1997, **56**:321-39.
27. J Rogers, JH Morrison: **Quantitative morphology and regional and laminar distributions of senile plaques in Alzheimer's disease**. *The Journal of neuroscience : the official journal of the Society for Neuroscience* 1985, **5**:2801-8.
28. JT Jarrett, EP Berger, PT Lansbury, Jr.: **The carboxy terminus of the beta amyloid protein is critical for the seeding of amyloid formation: implications for the pathogenesis of Alzheimer's disease**. *Biochemistry* 1993, **32**:4693-7.
29. YM Li: **Gamma-secretase: a catalyst of Alzheimer disease and signal transduction**. *Molecular interventions* 2001, **1**:198-207.
30. E Gowing, AE Roher, AS Woods, RJ Cotter, M Chaney, SP Little, MJ Ball: **Chemical characterization of A beta 17-42 peptide, a component of diffuse amyloid deposits of Alzheimer disease**. *The Journal of biological chemistry* 1994, **269**:10987-90.
31. T Iwatsubo, DM Mann, A Odaka, N Suzuki, Y Ihara: **Amyloid beta protein (A beta) deposition: A beta 42(43) precedes A beta 40 in Down syndrome**. *Annals of neurology* 1995, **37**:294-9.
32. H Yamaguchi, S Hirai, M Morimatsu, M Shoji, Y Harigaya: **Diffuse type of senile plaques in the brains of Alzheimer-type dementia**. *Acta neuropathologica* 1988, **77**:113-9.
33. F Tagliavini, G Giaccone, B Frangione, O Bugiani: **Preamyloid deposits in the cerebral cortex of patients with Alzheimer's disease and nondemented individuals**. *Neuroscience letters* 1988, **93**:191-6.
34. CA Lemere, JK Blusztajn, H Yamaguchi, T Wisniewski, TC Saido, DJ Selkoe: **Sequence of deposition of heterogeneous amyloid beta-peptides and APO E in Down syndrome: implications for initial events in amyloid plaque formation**. *Neurobiology of disease* 1996, **3**:16-32.
35. D Games, P Seubert: **The role of animal models in advancing amyloid-beta immunotherapy to the clinic**. *Alzheimers Res Ther* 2010, **2**:22.
36. D Morgan: **Cognitive Impairment in Transgenic Mouse Models of Amyloid Deposition.** In: *Animal Models of Cognitive Impairment* Edited by ED Levin, JJ Buccafusco. Boca Raton; 2006.
37. GD Van Vickle, CL Esh, WM Kalback, RL Patton, DC Luehrs, TA Kokjohn, FG Fifield, PE Fraser, D Westaway, J McLaurin, et al: **TgCRND8 amyloid precursor protein transgenic mice exhibit an altered gamma-secretase processing and an aggressive, additive**

**amyloid pathology subject to immunotherapeutic modulation**. *Biochemistry* 2007, **46**:10317-27.

38. S Dudal, P Krzywkowski, J Paquette, C Morissette, D Lacombe, P Tremblay, F Gervais: **Inflammation occurs early during the Abeta deposition process in TgCRND8 mice**. *Neurobiology of aging* 2004, **25**:861-71.
39. Q Guo, W Fu, BL Sopher, MW Miller, CB Ware, GM Martin, MP Mattson: **Increased vulnerability of hippocampal neurons to excitotoxic necrosis in presenilin-1 mutant knock-in mice**. *Nature medicine* 1999, **5**:101-6.
40. K Duff, C Eckman, C Zehr, X Yu, CM Prada, J Perez-tur, M Hutton, L Buee, Y Harigaya, D Yager, et al: **Increased amyloid-beta42(43) in brains of mice expressing mutant presenilin 1**. *Nature* 1996, **383**:710-3.
41. PA Barrow, RM Empson, SJ Gladwell, CM Anderson, R Killick, X Yu, JG Jefferys, K Duff: **Functional phenotype in transgenic mice expressing mutant human presenilin-1**. *Neurobiology of disease* 2000, **7**:119-26.
42. S Oddo, A Caccamo, JD Shepherd, MP Murphy, TE Golde, R Kayed, R Metherate, MP Mattson, Y Akbari, FM LaFerla: **Triple-transgenic model of Alzheimer's disease with plaques and tangles: intracellular Abeta and synaptic dysfunction**. *Neuron* 2003, **39**:409-21.
43. C Widmann, S Gibson, MB Jarpe, GL Johnson: **Mitogen-activated protein kinase: conservation of a three-kinase module from yeast to human**. *Physiological reviews* 1999, **79**:143-80.
44. G Pearson, F Robinson, T Beers Gibson, BE Xu, M Karandikar, K Berman, MH Cobb: **Mitogen-activated protein (MAP) kinase pathways: regulation and physiological functions**. *Endocrine reviews* 2001, **22**:153-83.
45. GL Johnson, R Lapadat: **Mitogen-activated protein kinase pathways mediated by ERK, JNK, and p38 protein kinases**. *Science* 2002, **298**:1911-2.
46. A Farooq, MM Zhou: **Structure and regulation of MAPK phosphatases**. *Cellular signalling* 2004, **16**:769-79.
47. M Gaestel, M Kracht: **Peptides as signaling inhibitors for mammalian MAP kinase cascades**. *Current pharmaceutical design* 2009, **15**:2471-80.
48. K Ono, J Han: **The p38 signal transduction pathway: activation and function**. *Cellular signalling* 2000, **12**:1-13.
49. S Kumar, PC McDonnell, RJ Gum, AT Hand, JC Lee, PR Young: **Novel homologues of CSBP/p38 MAP kinase: activation, substrate specificity and sensitivity to inhibition by pyridinyl imidazoles**. *Biochemical and biophysical research communications* 1997, **235**:533-8.
50. T Zarubin, J Han: **Activation and signaling of the p38 MAP kinase pathway**. *Cell research* 2005, **15**:11-8.
51. B Derijard, J Raingeaud, T Barrett, IH Wu, J Han, RJ Ulevitch, RJ Davis: **Independent human MAP-kinase signal transduction pathways defined by MEK and MKK isoforms**. *Science* 1995, **267**:682-5.
52. SJ Leevers, CJ Marshall: **Activation of extracellular signal-regulated kinase, ERK2, by p21ras oncoprotein**. *The EMBO journal* 1992, **11**:569-74.
53. CF Lai, L Chaudhary, A Fausto, LR Halstead, DS Ory, LV Avioli, SL Cheng: **Erk is essential for growth, differentiation, integrin expression, and cell function in human osteoblastic cells**. *Journal of Biological Chemistry* 2001, **276**:14443-14450.
54. MA Bogoyevitch, NW Court: **Counting on mitogen-activated protein kinases--ERKs 3, 4, 5, 6, 7 and 8**. *Cellular signalling* 2004, **16**:1345-54.

55. LA Tibbles, JR Woodgett: **The stress-activated protein kinase pathways**. *Cellular and molecular life sciences : CMLS* 1999, **55**:1230-54.
56. ZN Han, DL Boyle, LF Chang, B Bennett, M Karin, L Yang, AM Manning, GS Firestein: **C-Jun N-terminal kinase is required for metalloproteinase expression, and joint destruction in inflammatory arthritis**. *Journal of Clinical Investigation* 2001, **108**:73-81.
57. J Bijl-Westra: **Experimental studies on signal transduction pathways in rheumatoid arthritis.** Groningen: University of Groningen 2005.
58. A Porras, S Zuluaga, E Black, A Valladares, AM Alvarez, C Ambrosino, M Benito, AR Nebreda: **P38 alpha mitogen-activated protein kinase sensitizes cells to apoptosis induced by different stimuli**. *Molecular biology of the cell* 2004, **15**:922-33.
59. J Han, JD Lee, L Bibbs, RJ Ulevitch: **A MAP kinase targeted by endotoxin and hyperosmolarity in mammalian cells**. *Science* 1994, **265**:808-11.
60. Y Jiang, C Chen, Z Li, W Guo, JA Gegner, S Lin, J Han: **Characterization of the structure and function of a new mitogen-activated protein kinase (p38beta)**. *The Journal of biological chemistry* 1996, **271**:17920-6.
61. Z Li, Y Jiang, RJ Ulevitch, J Han: **The primary structure of p38 gamma: a new member of p38 group of MAP kinases**. *Biochemical and biophysical research communications* 1996, **228**:334-40.
62. XS Wang, K Diener, CL Manthey, S Wang, B Rosenzweig, J Bray, J Delaney, CN Cole, PY Chan-Hui, N Mantlo, et al: **Molecular cloning and characterization of a novel p38 mitogen-activated protein kinase**. *The Journal of biological chemistry* 1997, **272**:23668-74.
63. XS Wang, K Diener, CL Manthey, SW Wang, B Rosenzweig, J Bray, J Delaney, CN Cole, PY ChanHui, N Mantlo, et al: **Molecular cloning and characterization of a novel p38 mitogen-activated protein kinase**. *Journal of Biological Chemistry* 1997, **272**:23668-23674.
64. C Lechner, MA Zahalka, JF Giot, NPH Moller, A Ullrich: **ERK6, a mitogen-activated protein kinase involved in C2C12 myoblast differentiation**. *Proceedings of the National Academy of Sciences of the United States of America* 1996, **93**:4355-4359.
65. Y Jiang, H Gram, M Zhao, L New, J Gu, L Feng, F Di Padova, RJ Ulevitch, J Han: **Characterization of the structure and function of the fourth member of p38 group mitogen-activated protein kinases, p38delta**. *The Journal of biological chemistry* 1997, **272**:30122-8.
66. R Ben-Levy, S Hooper, R Wilson, HF Paterson, CJ Marshall: **Nuclear export of the stress-activated protein kinase p38 mediated by its substrate MAPKAP kinase-2**. *Current biology : CB* 1998, **8**:1049-57.
67. J Raingeaud, S Gupta, JS Rogers, M Dickens, J Han, RJ Ulevitch, RJ Davis: **Pro-inflammatory cytokines and environmental stress cause p38 mitogen-activated protein kinase activation by dual phosphorylation on tyrosine and threonine**. *The Journal of biological chemistry* 1995, **270**:7420-6.
68. M Takekawa, T Maeda, H Saito: **Protein phosphatase 2Calpha inhibits the human stress-responsive p38 and JNK MAPK pathways**. *The EMBO journal* 1998, **17**:4744-52.
69. S Kumar, J Boehm, JC Lee: **p38 map kinases: Key signalling molecules as therapeutic targets for inflammatory diseases**. *Nature Reviews Drug Discovery* 2003, **2**:717-726.
70. H Enslen, DM Brancho, RJ Davis: **Molecular determinants that mediate selective activation of p38 MAP kinase isoforms**. *Embo Journal* 2000, **19**:1301-1311.

71. H Enslen, J Raingeaud, RJ Davis: **Selective activation of p38 mitogen-activated protein (MAP) kinase isoforms by the MAP kinase kinases MKK3 and MKK6**. *The Journal of biological chemistry* 1998, **273**:1741-8.
72. PP Roux, J Blenis: **ERK and p38 MAPK-activated protein kinases: a family of protein kinases with diverse biological functions**. *Microbiology and molecular biology reviews : MMBR* 2004, **68**:320-44.
73. K Takeda, H Ichijo: **Neuronal p38 MAPK signalling: an emerging regulator of cell fate and function in the nervous system**. *Genes to cells : devoted to molecular & cellular mechanisms* 2002, **7**:1099-111.
74. P Wynne: **p38 mitogen-activated protein kinase: a novel modulator of hyperpolarization-activated cyclic nucleotide-gated channels and neuronal excitability**. *The Journal of neuroscience : the official journal of the Society for Neuroscience* 2006, **26**:11253-4.
75. Y Tan, J Rouse, A Zhang, S Cariati, P Cohen, MJ Comb: **FGF and stress regulate CREB and ATF-1 via a pathway involving p38 MAP kinase and MAPKAP kinase-2**. *The EMBO journal* 1996, **15**:4629-42.
76. MS Kim, HS So, JS Park, KM Lee, BS Moon, HS Lee, TY Kim, SK Moon, R Park: **Hwansodan protects PC12 cells against serum-deprivation-induced apoptosis via a mechanism involving Ras and mitogen-activated protein (MAP) kinase pathway**. *General Pharmacology-the Vascular System* 2000, **34**:227-235.
77. M Allen, L Svensson, M Roach, J Hambor, J McNeish, CA Gabel: **Deficiency of the stress kinase p38 alpha results in embryonic lethality: Characterization of the kinase dependence of stress responses of enzyme-deficient embryonic stem cells**. *Journal of Experimental Medicine* 2000, **191**:859-869.
78. A Kotlyarov, A Neininger, C Schubert, R Eckert, C Birchmeier, HD Volk, M Gaestel: **MAPKAP kinase 2 is essential for LPS-induced TNF-alpha biosynthesis**. *Nature Cell Biology* 1999, **1**:94-97.
79. D Caput, B Beutler, K Hartog, R Thayer, S Brownshimer, A Cerami: **Identification of a Common Nucleotide-Sequence in the 3'-Untranslated Region of Messenger-Rna Molecules Specifying Inflammatory Mediators**. *Proceedings of the National Academy of Sciences of the United States of America* 1986, **83**:1670-1674.
80. MJ Chae, HY Sung, EH Kim, M Lee, H Kwak, CH Chae, S Kim, WY Park: **Chemical inhibitors destabilize HuR binding to the AU-rich element of TNF-alpha mRNA**. *Exp Mol Med* 2009, **41**:824-31.
81. R Winzen, M Kracht, B Ritter, A Wilhelm, CYA Chen, AB Shyu, M Muller, M Gaestel, K Resch, H Holtmann: **The p38 MAP kinase pathway signals for cytokine-induced mRNA stabilization via MAP kinase-activated protein kinase 2 and an AU-rich region-targeted mechanism**. *Embo Journal* 1999, **18**:4969-4980.
82. A Cuenda, S Rousseau: **p38 MAP-kinases pathway regulation, function and role in human diseases**. *Biochimica et biophysica acta* 2007, **1773**:1358-75.
83. G Shaw, R Kamen: **A conserved AU sequence from the 3' untranslated region of GM-CSF mRNA mediates selective mRNA degradation**. *Cell* 1986, **46**:659-67.
84. Y Li, B Jiang, WY Ensign, PK Vogt, J Han: **Myogenic differentiation requires signalling through both phosphatidylinositol 3-kinase and p38 MAP kinase**. *Cellular signalling* 2000, **12**:751-7.
85. Z Wu, PJ Woodring, KS Bhakta, K Tamura, F Wen, JR Feramisco, M Karin, JY Wang, PL Puri: **p38 and extracellular signal-regulated kinases regulate the myogenic program at multiple steps**. *Molecular and cellular biology* 2000, **20**:3951-64.

86. G Sorci, F Riuzzi, AL Agneletti, C Marchetti, R Donato: **S100B inhibits myogenic differentiation and myotube formation in a RAGE-independent manner**. *Molecular and cellular biology* 2003, **23**:4870-81.
87. LA Greene, AS Tischler: **Establishment of a noradrenergic clonal line of rat adrenal pheochromocytoma cells which respond to nerve growth factor**. *Proceedings of the National Academy of Sciences of the United States of America* 1976, **73**:2424-8.
88. T Morooka, E Nishida: **Requirement of p38 mitogen-activated protein kinase for neuronal differentiation in PC12 cells**. *Journal of Biological Chemistry* 1998, **273**:24285-24288.
89. M Fukuda, Y Gotoh, T Tachibana, K Dell, S Hattori, Y Yoneda, E Nishida: **Induction of neurite outgrowth by MAP kinase in PC12 cells**. *Oncogene* 1995, **11**:239-44.
90. J Xing, JM Kornhauser, Z Xia, EA Thiele, ME Greenberg: **Nerve growth factor activates extracellular signal-regulated kinase and p38 mitogen-activated protein kinase pathways to stimulate CREB serine 133 phosphorylation**. *Molecular and cellular biology* 1998, **18**:1946-55.
91. A Pietersma, BC Tilly, N Gaestel, N deJong, JC Lee, JF Koster, W Sluiter: **P38 mitogen activated protein kinase regulates endothelial VCAM-1 expression at the post-transcriptional level**. *Biochemical and biophysical research communications* 1997, **230**:44-48.
92. GD Sharma, J He, HE Bazan: **p38 and ERK1/2 coordinate cellular migration and proliferation in epithelial wound healing: evidence of cross-talk activation between MAP kinase cascades**. *The Journal of biological chemistry* 2003, **278**:21989-97.
93. PA Klekotka, SA Santoro, MM Zutter: **alpha 2 integrin subunit cytoplasmic domain-dependent cellular migration requires p38 MAPK**. *The Journal of biological chemistry* 2001, **276**:9503-11.
94. R Vadlamudi, L Adam, A Talukder, J Mendelsohn, R Kumar: **Serine phosphorylation of paxillin by heregulin-beta1: role of p38 mitogen activated protein kinase**. *Oncogene* 1999, **18**:7253-64.
95. S Saika, Y Okada, T Miyamoto, O Yamanaka, Y Ohnishi, A Ooshima, CY Liu, D Weng, WW Kao: **Role of p38 MAP kinase in regulation of cell migration and proliferation in healing corneal epithelium**. *Investigative Ophthalmology & Visual Science* 2004, **45**:100-9.
96. S Rousseau, F Houle, J Landry, J Huot: **p38 MAP kinase activation by vascular endothelial growth factor mediates actin reorganization and cell migration in human endothelial cells**. *Oncogene* 1997, **15**:2169-77.
97. JES Torres, V Chaparro-Huerta, MCR Cervantres, R Montes-Gonzalez, MEF Soto, C Beas-Zarate: **Neuronal cell death due to glutamate excitotocity is mediated by P38 activation in the rat cerebral cortex**. *Neuroscience letters* 2006, **403**:233-238.
98. K Chen, MD Maines: **Nitric oxide induces heme oxygenase-1 via mitogen-activated protein kinases ERK and p38**. *Cellular and molecular biology* 2000, **46**:609-17.
99. T Wada, JM Penninger: **Mitogen-activated protein kinases in apoptosis regulation**. *Oncogene* 2004, **23**:2838-49.
100. RA Salmon, IN Foltz, PR Young, JW Schrader: **The p38 mitogen-activated protein kinase is activated by ligation of the T or B lymphocyte antigen receptors, Fas or CD40, but suppression of kinase activity does not inhibit apoptosis induced by antigen receptors**. *Journal of Immunology* 1997, **159**:5309-17.
101. J Zhang, KV Salojin, JX Gao, MJ Cameron, I Bergerot, TL Delovitch: **p38 mitogen-activated protein kinase mediates signal integration of TCR/CD28 costimulation in primary murine T cells**. *Journal of Immunology* 1999, **162**:3819-29.

102. JM Park, FR Greten, ZW Li, M Karin: **Macrophage apoptosis by anthrax lethal factor through p38 MAP kinase inhibition**. *Science* 2002, **297**:2048-51.
103. A Roulston, C Reinhard, P Amiri, LT Williams: **Early activation of c-Jun N-terminal kinase and p38 kinase regulate cell survival in response to tumor necrosis factor alpha**. *The Journal of biological chemistry* 1998, **273**:10232-9.
104. Y Nagata, K Todokoro: **Requirement of activation of JNK and p38 for environmental stress-induced erythroid differentiation and apoptosis and of inhibition of ERK for apoptosis**. *Blood* 1999, **94**:853-63.
105. A Yoshimura: **Signal transduction of inflammatory cytokines and tumor development**. *Cancer science* 2006, **97**:439-47.
106. C Ambrosino, AR Nebreda: **Cell cycle regulation by p38 MAP kinases**. *Biology of the cell / under the auspices of the European Cell Biology Organization* 2001, **93**:47-51.
107. CH McGowan, P Russell: **The DNA damage response: sensing and signaling**. *Current opinion in cell biology* 2004, **16**:629-33.
108. R Sanchez-Prieto, JM Rojas, Y Taya, JS Gutkind: **A role for the p38 mitogen-acitvated protein kinase pathway in the transcriptional activation of p53 on genotoxic stress by chemotherapeutic agents**. *Cancer research* 2000, **60**:2464-72.
109. EF Wagner, AR Nebreda: **Signal integration by JNK and p38 MAPK pathways in cancer development**. *Nature reviews. Cancer* 2009, **9**:537-49.
110. Y Wang, B Su, VP Sah, JH Brown, J Han, KR Chien: **Cardiac hypertrophy induced by mitogen-activated protein kinase kinase 7, a specific activator for c-Jun NH2-terminal kinase in ventricular muscle cells**. *The Journal of biological chemistry* 1998, **273**:5423-6.
111. D Zechner, DJ Thuerauf, DS Hanford, PM McDonough, CC Glembotski: **A role for the p38 mitogen-activated protein kinase pathway in myocardial cell growth, sarcomeric organization, and cardiac-specific gene expression**. *The Journal of cell biology* 1997, **139**:115-27.
112. M Zheng, C Reynolds, SH Jo, R Wersto, Q Han, RP Xiao: **Intracellular acidosis-activated p38 MAPK signaling and its essential role in cardiomyocyte hypoxic injury**. *The FASEB journal : official publication of the Federation of American Societies for Experimental Biology* 2005, **19**:109-11.
113. JK Kim, A Pedram, M Razandi, ER Levin: **Estrogen prevents cardiomyocyte apoptosis through inhibition of reactive oxygen species and differential regulation of p38 kinase isoforms**. *The Journal of biological chemistry* 2006, **281**:6760-7.
114. K Hensley, RA Floyd, NY Zheng, R Nael, KA Robinson, X Nguyen, QN Pye, CA Stewart, J Geddes, WR Markesbery, et al: **p38 kinase is activated in the Alzheimer's disease brain**. *Journal of neurochemistry* 1999, **72**:2053-8.
115. M Koistinaho, MI Kettunen, G Goldsteins, R Keinanen, A Salminen, M Ort, J Bures, D Liu, RA Kauppinen, LS Higgins, et al: **Beta-amyloid precursor protein transgenic mice that harbor diffuse A beta deposits but do not form plaques show increased ischemic vulnerability: role of inflammation**. *Proceedings of the National Academy of Sciences of the United States of America* 2002, **99**:1610-5.
116. X Cao, L Rui, PR Pennington, J Chlan-Fourney, Z Jiang, Z Wei, XM Li, DE Edmondson, DD Mousseau: **Serine 209 resides within a putative p38(MAPK) consensus motif and regulates monoamine oxidase-A activity**. *Journal of neurochemistry* 2009, **111**:101-10.
117. C Atzori, B Ghetti, R Piva, AN Srinivasan, P Zolo, MB Delisle, SS Mirra, A Migheli: **Activation of the JNK/p38 pathway occurs in diseases characterized by tau protein pathology and is related to tau phosphorylation but not to apoptosis**. *Journal of neuropathology and experimental neurology* 2001, **60**:1190-7.

118. MG Giovannini, F Cerbai, A Bellucci, C Melani, C Grossi, C Bartolozzi, D Nosi, F Casamenti: **Differential activation of mitogen-activated protein kinase signalling pathways in the hippocampus of CRND8 transgenic mouse, a model of Alzheimer's disease**. *Neuroscience* 2008, **153**:618-33.
119. X Zhu, CA Rottkamp, A Hartzler, Z Sun, A Takeda, H Boux, S Shimohama, G Perry, MA Smith: **Activation of MKK6, an upstream activator of p38, in Alzheimer's disease**. *Journal of neurochemistry* 2001, **79**:311-8.
120. C Feijoo, DG Campbell, R Jakes, M Goedert, A Cuenda: **Evidence that phosphorylation of the microtubule-associated protein Tau by SAPK4/p38delta at Thr50 promotes microtubule assembly**. *Journal of cell science* 2005, **118**:397-408.
121. SM Jenkins, M Zinnerman, C Garner, GV Johnson: **Modulation of tau phosphorylation and intracellular localization by cellular stress**. *The Biochemical journal* 2000, **345 Pt 2**:263-70.
122. B Langguth, R Salvi, AB Elgoyhen: **Emerging pharmacotherapy of tinnitus**. *Expert opinion on emerging drugs* 2009, **14**:687-702.
123. M Ankarcrona, K Hultenby: **Presenilin-1 is located in rat mitochondria**. *Biochemical and biophysical research communications* 2002, **295**:766-70.
124. DS Tzeng, CC Chien, FW Lung, CY Yang: **MAOA gene polymorphisms and response to mirtazapine in major depression**. *Human psychopharmacology* 2009, **24**:293-300.
125. JM Ringman, C Diaz-Olavarrieta, Y Rodriguez, M Chavez, F Paz, J Murrell, MA Macias, M Hill, C Kawas: **Female preclinical presenilin-1 mutation carriers unaware of their genetic status have higher levels of depression than their non-mutation carrying kin**. *Journal of neurology, neurosurgery, and psychiatry* 2004, **75**:500-2.
126. AA Culbert, SD Skaper, DR Howlett, NA Evans, L Facci, PE Soden, ZM Seymour, F Guillot, M Gaestel, JC Richardson: **MAPK-activated protein kinase 2 deficiency in microglia inhibits pro-inflammatory mediator release and resultant neurotoxicity. Relevance to neuroinflammation in a transgenic mouse model of Alzheimer disease**. *The Journal of biological chemistry* 2006, **281**:23658-67.
127. SA Frautschy, F Yang, M Irrizarry, B Hyman, TC Saido, K Hsiao, GM Cole: **Microglial response to amyloid plaques in APPsw transgenic mice**. *The American journal of pathology* 1998, **152**:307-17.
128. A Bellucci, MC Rosi, C Grossi, A Fiorentini, I Luccarini, F Casamenti: **Abnormal processing of tau in the brain of aged TgCRND8 mice**. *Neurobiology of disease* 2007, **27**:328-38.
129. SH Lee, J Park, Y Che, PL Han, JK Lee: **Constitutive activity and differential localization of p38alpha and p38beta MAPKs in adult mouse brain**. *Journal of neuroscience research* 2000, **60**:623-31.
130. JG Park, Y Yuk, H Rhim, SY Yi, YS Yoo: **Role of p38 MAPK in the regulation of apoptosis signaling induced by TNF-alpha in differentiated PC12 cells**. *Journal of biochemistry and molecular biology* 2002, **35**:267-72.
131. T Morooka, E Nishida: **Requirement of p38 mitogen-activated protein kinase for neuronal differentiation in PC12 cells**. *The Journal of biological chemistry* 1998, **273**:24285-8.
132. N Juretic, JF Santibanez, C Hurtado, J Martinez: **ERK 1,2 and p38 pathways are involved in the proliferative stimuli mediated by urokinase in osteoblastic SaOS-2 cell line**. *Journal of cellular biochemistry* 2001, **83**:92-8.
133. X Zhu, AK Raina, HG Lee, M Chao, A Nunomura, M Tabaton, RB Petersen, G Perry, MA Smith: **Oxidative stress and neuronal adaptation in Alzheimer disease: the role of SAPK pathways**. *Antioxidants & redox signaling* 2003, **5**:571-6.

134. MA Chishti, DS Yang, C Janus, AL Phinney, P Horne, J Pearson, R Strome, N Zuker, J Loukides, J French, et al: **Early-onset amyloid deposition and cognitive deficits in transgenic mice expressing a double mutant form of amyloid precursor protein 695**. *The Journal of biological chemistry* 2001, **276**:21562-70.
135. GB Frisoni, A Prestia, PE Rasser, M Bonetti, PM Thompson: **In vivo mapping of incremental cortical atrophy from incipient to overt Alzheimer's disease**. *Journal of neurology* 2009, **256**:916-24.
136. I Yakushev, A Hammers, A Fellgiebel, I Schmidtmann, A Scheurich, HG Buchholz, J Peters, P Bartenstein, K Lieb, M Schreckenberger: **SPM-based count normalization provides excellent discrimination of mild Alzheimer's disease and amnestic mild cognitive impairment from healthy aging**. *NeuroImage* 2009, **44**:43-50.
137. MR D'Andrea, RG Nagele: **Morphologically distinct types of amyloid plaques point the way to a better understanding of Alzheimer's disease pathogenesis**. *Biotechnic & histochemistry : official publication of the Biological Stain Commission* 2010, **85**:133-47.
138. B Puig, T Gomez-Isla, E Ribe, M Cuadrado, B Torrejon-Escribano, E Dalfo, I Ferrer: **Expression of stress-activated kinases c-Jun N-terminal kinase (SAPK/JNK-P) and p38 kinase (p38-P), and tau hyperphosphorylation in neurites surrounding betaA plaques in APP Tg2576 mice**. *Neuropathology and applied neurobiology* 2004, **30**:491-502.
139. JJ Pei, E Braak, H Braak, I Grundke-Iqbal, K Iqbal, B Winblad, RF Cowburn: **Localization of active forms of C-jun kinase (JNK) and p38 kinase in Alzheimer's disease brains at different stages of neurofibrillary degeneration**. *Journal of Alzheimer's disease : JAD* 2001, **3**:41-48.
140. MJ Savage, YG Lin, JR Ciallella, DG Flood, RW Scott: **Activation of c-Jun N-terminal kinase and p38 in an Alzheimer's disease model is associated with amyloid deposition**. *The Journal of neuroscience : the official journal of the Society for Neuroscience* 2002, **22**:3376-85.
141. D Caput, B Beutler, K Hartog, R Thayer, S Brown-Shimer, A Cerami: **Identification of a common nucleotide sequence in the 3'-untranslated region of mRNA molecules specifying inflammatory mediators**. *Proc Natl Acad Sci U S A* 1986, **83**:1670-4.
142. AR Simard, D Soulet, G Gowing, JP Julien, S Rivest: **Bone marrow-derived microglia play a critical role in restricting senile plaque formation in Alzheimer's disease**. *Neuron* 2006, **49**:489-502.
143. J El Khoury, M Toft, SE Hickman, TK Means, K Terada, C Geula, AD Luster: **Ccr2 deficiency impairs microglial accumulation and accelerates progression of Alzheimer-like disease**. *Nature medicine* 2007, **13**:432-8.
144. A Nimmerjahn, F Kirchhoff, F Helmchen: **Resting microglial cells are highly dynamic surveillants of brain parenchyma in vivo**. *Science* 2005, **308**:1314-8.
145. R Hua, W Walz: **Minocycline treatment prevents cavitation in rats after a cortical devascularizing lesion**. *Brain research* 2006, **1090**:172-81.
146. A Majumdar, D Cruz, N Asamoah, A Buxbaum, I Sohar, P Lobel, FR Maxfield: **Activation of microglia acidifies lysosomes and leads to degradation of Alzheimer amyloid fibrils**. *Molecular biology of the cell* 2007, **18**:1490-6.
147. T Bolmont, F Haiss, D Eicke, R Radde, CA Mathis, WE Klunk, S Kohsaka, M Jucker, ME Calhoun: **Dynamics of the microglial/amyloid interaction indicate a role in plaque maintenance**. *The Journal of neuroscience : the official journal of the Society for Neuroscience* 2008, **28**:4283-92.
148. V Boissonneault, M Filali, M Lessard, J Relton, G Wong, S Rivest: **Powerful beneficial effects of macrophage colony-stimulating factor on beta-amyloid deposition and**

**cognitive impairment in Alzheimer's disease**. *Brain : a journal of neurology* 2009, **132**:1078-92.

149. N Choucair-Jaafar, V Laporte, R Levy, P Poindron, Y Lombard, JP Gies: **Complement receptor 3 (CD11b/CD18) is implicated in the elimination of beta-amyloid peptides**. *Fundamental & clinical pharmacology* 2011, **25**:115-22.
150. KD Bornemann, KH Wiederhold, C Pauli, F Ermini, M Stalder, L Schnell, B Sommer, M Jucker, M Staufenbiel: **Abeta-induced inflammatory processes in microglia cells of APP23 transgenic mice**. *The American journal of pathology* 2001, **158**:63-73.
151. BP Kennedy, MG Ziegler, M Alford, LA Hansen, LJ Thal, E Masliah: **Early and persistent alterations in prefrontal cortex MAO A and B in Alzheimer's disease**. *J Neural Transm* 2003, **110**:789-801.
152. WJ Burke, SW Li, CA Schmitt, P Xia, HD Chung, KN Gillespie: **Accumulation of 3,4-dihydroxyphenylglycolaldehyde, the neurotoxic monoamine oxidase A metabolite of norepinephrine, in locus ceruleus cell bodies in Alzheimer's disease: mechanism of neuron death**. *Brain Res* 1999, **816**:633-7.
153. V Chan-Palay, M Hochli, E Savaskan, G Hungerecker: **Calbindin D-28k and monoamine oxidase A immunoreactive neurons in the nucleus basalis of Meynert in senile dementia of the Alzheimer type and Parkinson's disease**. *Dementia* 1993, **4**:1-15.